Aluminum Laser Additive Manufacturing: A Review on Challenges and Opportunities Through the Lens of Sustainability

applied sciences

MDPI

Review

Aluminum Laser Additive Manufacturing: A Review on Challenges and Opportunities Through the Lens of Sustainability

Mohammad Javad Yadegari, Alessandra Martucci *, Sara Biamino, Daniele Ugues, Laura Montanaro, Paolo Fino and Mariangela Lombardi *

Department of Applied Science and Technology, Politecnico di Torino, Corso Duca Degli Abruzzi 24, 10129 Turin, Italy; mohammad.yadegari@polito.it (M.J.Y.); sara.biamino@polito.it (S.B.); daniele.ugues@polito.it (D.U.); laura.montanaro@polito.it (L.M.); paolo.fino@polito.it (P.F.)
* Correspondence: alessandra.martucci@polito.it (A.M.); mariangela.lombardi@polito.it (M.L.)

Abstract: The manufacturing sector is a major contributor to global energy consumption and greenhouse gas emissions, positioning sustainability as a critical priority. Aluminum, valued for its lightweight and recyclable properties, plays a vital role in advancing energy-efficient solutions across transportation and aerospace industries. The processing of aluminum alloys through laser-based powder bed fusion of metals (PBF-LB/M), a cutting-edge additive manufacturing technology, enhances sustainability by optimizing material usage and enabling innovative lightweight designs. Based on the published literature, the present study analyzed the ecological impacts of aluminum PBF-LB/M manufacturing through life cycle assessment, circular economy principles, and eco-design strategies, identifying opportunities to reduce environmental footprints. The study also stated the critical challenges, such as the high energy demands of the aluminum PBF-LB/M process and its scalability limitations. Potential sustainable solutions were discussed starting from powder production techniques, as well as optimized processes and post-processing strategies. By adopting an interdisciplinary approach, this research highlighted the pivotal role of PBFed aluminum alloys in achieving sustainable manufacturing goals. It provided actionable insights to drive innovation and resilience in industrial applications, offering a roadmap for balancing environmental stewardship with the demands of high-performance standards.

Keywords: additive manufacturing; sustainability; laser powder bed fusion; aluminum alloys; productivity; lightweight design

Academic Editors: Zhonghua Sun and Mauro Vaccarezza

Received: 31 December 2024
Revised: 14 February 2025
Accepted: 15 February 2025
Published: 19 February 2025

Citation: Yadegari, M.J.; Martucci, A.; Biamino, S.; Ugues, D.; Montanaro, L.; Fino, P.; Lombardi, M. Aluminum Laser Additive Manufacturing: A Review on Challenges and Opportunities Through the Lens of Sustainability. *Appl. Sci.* **2025**, *15*, 2221. https://doi.org/10.3390/app15042221

1. Introduction

Global warming remains one of the most pressing environmental challenges, driven largely by the rising concentration of greenhouse gases in the atmosphere. Among these, CO_2 emissions from fossil-based industrial activities, including material production, manufacturing, and transportation, are significant contributors. As a result, sustainability has become a global priority, particularly in the manufacturing sector, which is a major energy consumer and carbon dioxide emitter. This sector faces growing pressure to decarbonize while meeting increasing demands for advanced materials and technologies [1–4]. Sustainable development, as conceptualized by the Brundtland Commission, is grounded in three interconnected dimensions: economic, social, and environmental [5]. These dimensions are assessed using specific metrics: economic impact through cost, social impact qualitatively, and environmental impact via measures such as energy consumption and carbon emissions [6,7]. This framework aligns with the "Three P" model, People, Planet, and Profit (or Prosperity), and the triple bottom line approach, which considers these dimensions as

distinct yet interdependent forms of capital. Economic capital represents financial value, natural capital refers to environmental resources, and human capital addresses societal well-being [8].

Additive Manufacturing (AM), particularly laser-based powder bed fusion of metals (PBF-LB/M), has emerged as a cornerstone of sustainable manufacturing. AM offers transformative potential by enabling efficient material utilization, reducing production waste, and supporting circular economy principles. These characteristics make AM an ideal solution for producing lightweight, high-performance components that align with sustainability goals [9,10].

Aluminum plays a pivotal role in energy transitions and lightweighting applications, especially in transportation and aerospace. Known for its high strength-to-weight ratio, durability, and recyclability, aluminum is a key material for sustainability [11,12]. Recycling aluminum requires only 5% of the energy needed for primary production, significantly lowering carbon emissions and energy consumption [13]. Its lightweight properties further enhance energy efficiency, resulting in reduced fuel consumption and emissions in automotive and aerospace applications. Beyond transportation, aluminum contributes to energy-efficient buildings, solar panels, and electric vehicles, solidifying its importance in advancing global efficiency and eco-friendly industries [14–17].

Processing aluminum alloys via PBF-LB/M presents significant opportunities to minimize environmental impacts in sectors where weight reduction is critical, such as the automotive and aerospace sectors [9]. As a driving force of the Fourth Industrial Revolution, PBF-LB/M enables the production of complex mechanical and structural components. Its layer-by-layer fabrication process offers unparalleled design freedom, superior material optimization, and the ability to produce intricate geometries. Additionally, PBF-LB/M supports the development of multi-part assemblies, functionally graded materials, and advanced meta-materials, capabilities often beyond the reach of traditional manufacturing [18–20]. The technology rapid adoption across industries such as aerospace, automotive, healthcare, and consumer goods underscores its transformative potential.

Although the PBF-LB/M improved material efficiency and other advantages, aluminum processing through this promising AM technology remains energy-intensive. The energy demands associated with metal powder production, spanning feedstock melting, atomization, powder collection, classification, and secure storage, are significant contributors to the environmental footprint of PBF-LB/M [8,21,22]. This paper investigates the environmental sustainability of PBF-LB/M in aluminum alloy production, with a focus on strategies to enhance ecological performance across key areas, including feedstock preparation, processing, and post-processing techniques. By prioritizing waste reduction and energy efficiency, the research aims to improve both the profitability and performance of PBF-LB/M.

The rest of the paper is organized as follows. Section 2 addresses global environmental challenges, highlighting the role of aluminum in sustainable manufacturing and positioning PBF-LB/M as a key solution. The ecological impacts are analyzed using Life Cycle Assessment (LCA), circular economy principles, and eco-design approaches, with a particular emphasis on the sustainability needs of the mobility sector. Section 3 examines feedstock sustainability through environmentally conscious powder fabrication methods, secondary raw materials incorporation, and powder reuse strategies to minimize waste. Section 4 analyzes the PBF-LB/M process from two perspectives: the development of lightweight aluminum compositions and structural optimization using techniques such as topology optimization and latticing, as well as process improvements aimed at enhancing productivity, quality, and component longevity through parameter optimization and advanced monitoring systems. Finally, Section 5 discusses sustainable post-processing methods,

focusing on efficient heat treatment and surface finishing techniques to reduce reliance on extensive post-processing while maintaining high-performance outcomes. Figure 1 illustrates the overall structure of this review.

Figure 1. Structure of this review.

2. Ecological Impacts

Global warming, primarily driven by greenhouse gas emissions, remains one of the most pressing global challenges. Industrial production and manufacturing are significant contributors, representing a substantial share of global energy consumption and CO_2 emissions. The decarbonization of industrial activity is particularly challenging due to the high cost and developmental stage of many low-carbon solutions, as well as the long operational lifespans of industrial assets, which limit their replacement frequency. According to the International Energy Agency (IEA) [23], industrial activity accounted for 37% (166 EJ) of global energy consumption in 2022, resulting in approximately 25% (9.0 Gt) of worldwide CO_2 emissions. In particular, in 2022, the aluminum sector emitted approximately 0.27 Gt of CO_2, representing 0.7% of global emissions and nearly 3% of direct industrial emissions (Figure 2). This trend has been exacerbated by rising aluminum production, driven by population growth and economic expansion. These estimates align with the most recent and finalized data available in the database of annual time series on greenhouse gas emissions from energy, which is updated biannually, with the latest comprehensive dataset covering the year 2022.

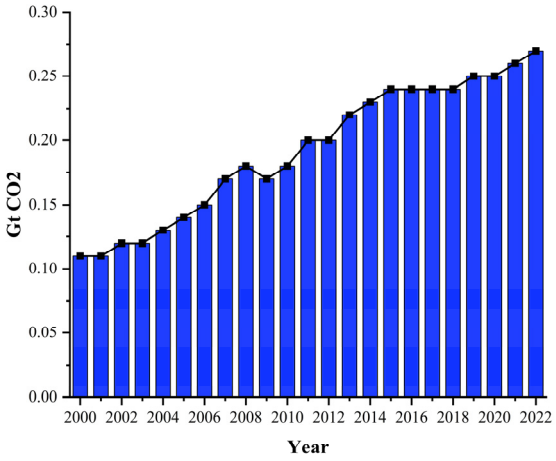

Figure 2. CO_2 emissions from aluminum industry (based on [23]).

A part of Agenda 2030 for Sustainable Development, adopted by the United Nations in 2015, provides a comprehensive action plan to address global issues related to the energy consumption of industrial activities. To facilitate organizational alignment with the SDGs, the ISO/UNDP PAS 53002 guidelines outline strategies for systematically managing and enhancing contributions to sustainable development across operations [24]. Aligned with the Agenda 2030, the Paris Agreement, adopted in 2016, united 195 countries in a commitment to combat global warming. Its primary objective is to limit global temperature rise to well below 2 °C above pre-industrial levels, with an aspirational target of 1.5 °C. Achieving these goals requires rapid and substantial reductions in greenhouse gas emissions, with net-zero emissions by 2050 as a cornerstone objective. Limiting warming to 1.5 °C necessitates a 50% reduction in global emissions by 2030 and a reduction of over 90% by 2050, allowing minimal offsets for the remaining emissions [25,26].

Based on the IEA report on transport energy systems [27], the transport sector accounts for approximately 22% (8.0 Gt) of global CO_2 emissions. To achieve the net-zero emissions target by 2050, emissions from this sector must be reduced by approximately 25%, reaching around 6 Gt by 2030, despite continued growth in transport demand. This necessitates an annual emissions reduction of more than 3% through 2030. Road transport, encompassing vehicles such as cars and trucks, accounts for approximately 16% of global energy-related CO_2 emissions, equivalent to 5.8 Gt CO_2. Private cars and vans alone contribute to over 25% of global oil consumption. Although aviation represents a smaller share of total emissions, it is one of the most challenging sectors to decarbonize. In 2022, aviation accounted for 2% of global energy-related CO_2 emissions, totaling nearly 800 Mt CO_2. Over recent decades, aviation emissions have grown faster than other modes of transport, such as rail, road, and shipping. In the CRU Consulting report titled Opportunities for Aluminum in a Post-COVID Economy, prepared for the International Aluminum Institute [28], the global demand for aluminum is projected to grow significantly, increasing by 33.3 Mt from 86.2 Mt in 2020 to 119.5 Mt in 2030. The transportation sector is anticipated to drive the largest absolute growth, contributing approximately 35% of this increase. Aluminum consumption in this sector is forecasted to rise from 19.9 Mt in 2020 to 31.7 Mt in 2030. This growth underscores the critical role of aluminum in enabling the development of lighter and more efficient vehicle designs, solidifying its position as a key material in advancing sustainability within the transportation industry.

To align with net-zero objectives, stakeholders, including manufacturers, consumers, and policymakers, must enhance more sustainable aluminum processing technologies and improve aluminum scrap collection, sorting, and recycling. These coordinated efforts are essential for reducing waste, lowering emissions across the supply chain, and achieving global climate goals [11]. Among more sustainable aluminum processing technologies, AM emerges as a promising solution. AM is a transformative approach to producing complex mechanical and structural components, positioning itself as a major catalyst in the Fourth Industrial Revolution, also known as digital industrial transformation. AM significantly reduces material waste through its "near-net-shape" approach, producing components with complex geometries while using only the necessary material. Furthermore, the design optimization enabled by AM allows for the creation of lighter and more efficient components, contributing to energy savings in industries. It further facilitates the creation of multi-part assemblies, functionally graded materials, and meta-materials, capabilities often challenging or unattainable through conventional manufacturing. Consequently, AM is not only redefining conventional manufacturing paradigms but also advancing sustainable development by minimizing resource usage and promoting localized production models that help lower the carbon footprint associated with extended supply chains.

Although the material efficiency and supply chain shortening that characterize AM bear the potential to advance the sustainability of these processes over traditional manufacturing methods, much of additive technology is energy intensive and often has a higher carbon footprint per kilogram of final product than traditional manufacturing techniques [8]. The PBF-LB/M additive technology is particularly critical from a sustainability perspective due to its environmental impact, which is contributed to by the energy-intensive production of metal powders, the significant consumption of inert gas during processing, and the challenges in recycling unused powder. To evaluate and mitigate these impacts, Product Carbon Footprint calculations, following the ISO 14067 standard [29], are a valid tool to quantify the CO_2 emissions (expressed in kg CO_2 equivalent) linked to the production of each kilogram of metal powder. Additionally, ISO 14040 [30], which provides guidelines for LCA, can be useful to assess the total environmental impact of products throughout their entire life cycle, from raw material extraction to disposal or recycling.

LCA is a comprehensive framework for evaluating the environmental impacts of a product system, such as energy consumption and CO_2 emissions, across various phases of its life cycle. It systematically analyzes inputs and outputs throughout the product lifespan and interprets the results to support sustainable decision-making. A PBFed product life cycle typically consists of five phases: material production, which involves raw material extraction and processing; manufacturing, which focuses on the fabrication of parts or components; transport, which includes the distribution of parts or products to assembly sites or end-users; use, which covers operational impacts during the product usage phase; and disposal, which entails end-of-life management, including recycling or landfill. LCA can be adapted to different system boundaries. Cradle-to-grave assessments include all phases from raw material extraction to end-of-life disposal, while cradle-to-gate studies focus on material production and manufacturing, and gate-to-gate analyzes examine only the manufacturing process. Figure 3 illustrates the system boundaries and phases of the product life cycle specific to PBF-LB/M.

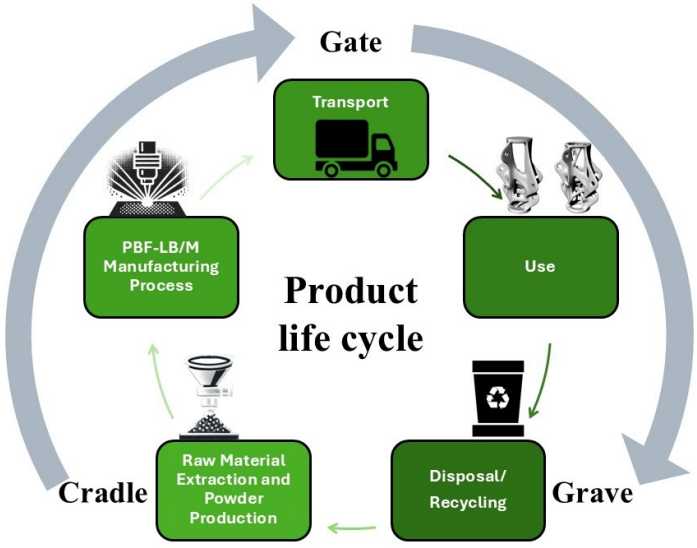

Figure 3. Life cycle of a component produced by PBF-LB/M.

Conducting an LCA provides a data-driven evaluation of the environmental impacts associated with using advanced and lightweight materials like novel aluminum alloys in PBF-LB/M [31]. Life cycle inventory data for PBF-LB/M components is typically derived from industrial printing practices or academic studies. Huang et al. [32] estimate that the energy consumption of Al alloy AM technologies during the cradle-to-gate phase ranges from 73 to 94 MJ/kg, with associated CO_2 emissions between 5.0 and 6.4 kg CO_2/kg.

However, these values can rise significantly, reaching 374 to 520 MJ/kg and 25.4 to 35.4 kg CO_2/kg, depending on the electricity system utilized and its energy efficiency. Weiss et al. [33] proposed a comprehensive life cycle model for the production of components utilizing AlSi10Mg powder. As depicted in Figure 4, the life cycle inventory data for the scenario involving the production of four impellers per build job via PBF-LB/M indicates a total energy consumption of 775.6 kWh per build. Across the manufacturing of 7360 components, the process generates a cumulative emission of 304,309 kg CO_2-eq, corresponding to an average emission of 41.35 kg CO_2-eq per component.

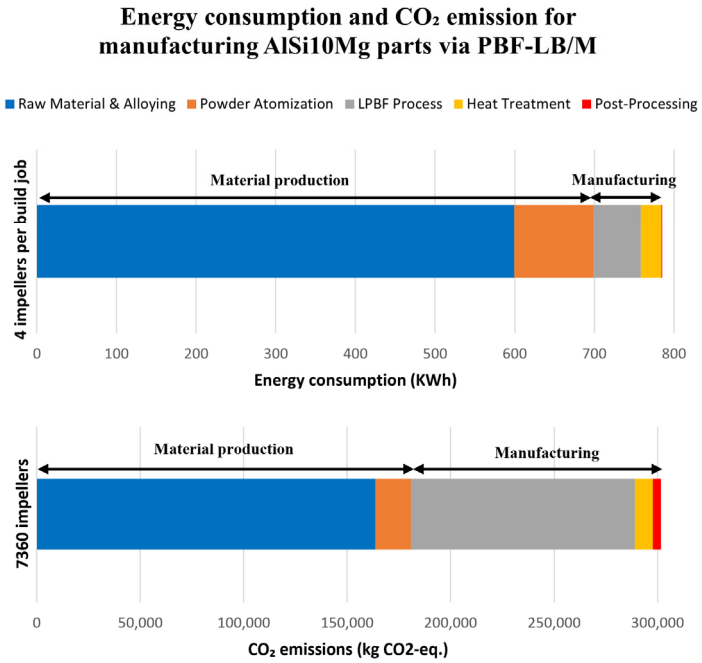

Figure 4. Life cycle inventory and impact assessment of manufacturing impellers via PBF-LB/M (based on data in [33]).

Ingarao et al. [34] compared the environmental impacts of aluminum parts produced by PBF-LB/M with traditional machining and forming processes. Utilizing LCA techniques, the study assesses each method in terms of material production, processing, and weight reduction potential. The findings reveal that PBF-LB/M offers a sustainable advantage primarily in scenarios involving high geometric complexity, significant weight reduction, or applications within transportation systems. Priarone et al. [35] investigate the influence of design choices on the environmental sustainability of PBF-LB/M processes, utilizing LCA techniques on a bearing bracket produced with AlSi10Mg. Critical design elements, such as topological optimization and support structure configuration, significantly impact energy consumption and CO_2 emissions throughout the product life cycle. The study findings indicate that carefully optimized design can achieve substantial environmental benefits, particularly in the operational phase of lightweight components used in transportation applications.

Together, LCA, the circular economy, and eco-design form a holistic framework that drives sustainable practices in AM processes. The circular economy provides an essential framework for minimizing waste and maximizing resource use by maintaining materials, products, and components in continuous cycles. Unlike the linear "take, make, dispose" model, the circular economy aims to "close the loop", enhancing resource productivity and reducing reliance on virgin materials. This approach emphasizes recycling, repurposing, and remanufacturing and supports sustainable production and consumption. Metals are particularly well-suited for advancing a circular economy, owing to their superior recyclability and potential for repeated reuse without significant degradation. In PBF-LB/M,

circular economy principles align closely with manufacturing needs, as they support the recovery, recycling, and reuse of metal powders. Unused or excess powder can be collected, refined, and reintegrated into production, creating closed-loop systems and promoting sustainable resource management [10,36]. Eco-design has emerged as a strategic approach to embedding sustainability at the design stage, maximizing environmental benefits early in product development. In PBF-LB/M, eco-design leverages the flexibility of technology design to create more sustainable components. The layer-by-layer fabrication inherent in PBF-LB/M enables complex geometries that conserve material without compromising performance, advancing eco-design objectives and reinforcing the shift toward sustainable manufacturing practices.

Employing a holistic approach, Peng et al. [37] analyzed the life cycle impacts of PBF-LB/M compared to conventional manufacturing for a hydraulic valve body, examining the roles of design, material preparation, and fabrication. Their study revealed that, without design optimization, the AM process could offer a 37.42% reduction in environmental impact relative to conventional techniques. By exploiting the optimization of the PBF-LB/M design, a further impact reduction of 10–23% was achieved. Salmi et al. [38] present a multi-criteria decision-making framework to compare PBF-LB/M with CNC machining and high-pressure die casting. Through a case study on an aerospace bracket made from Al2139, the framework demonstrates the suitability of AM for small to medium production runs of up to 100 units.

3. Feedstock

3.1. Powder Production

The powder preparation stage represents the most significant environmental impact in PBF-LB/M, primarily driven by the high electricity demands associated with the process, contributing to substantial fossil fuel depletion [39,40]. The carbon footprint of metal powder production is largely influenced by the choice of feedstock, with each option exhibiting a distinct environmental impact. These variations are primarily driven by factors such as the energy required for raw material extraction, subsequent processing, and transportation-related emissions.

The primary manufacturing methods for AM powders include water atomization (WA), gas atomization (GA), plasma atomization, centrifugal atomization, and various other specialized metal powder production techniques. WA represents the highest-volume production process. In this method, a stream of molten metal is fragmented by high-pressure water. Due to the rapid cooling, the resulting metal droplets do not have sufficient time to spheroidize, leading to irregular particle shapes. Under optimized processing conditions, however, non-spherical powders can be used effectively in AM to produce parts with mechanical properties comparable to those of high-strength wrought materials, significantly broadening the range of viable raw materials [41,42]. Research by Kruzhanov and Arnhold [43] indicates that WA for powder production typically consumes around 6.48 MJ/kg (1.8 kWh/kg), with energy requirements significantly influenced by the melting point of the metal being processed. Conversely, GA utilizes a high-pressure gas stream to break a molten metal stream into fine droplets. These droplets then free-fall through a chamber, solidifying before collection. Surface tension during the fall allows the droplets to assume a spherical form. The alloy composition is prepared in a melting furnace using various raw materials, providing flexibility in formulation. This process yields powders with exceptional purity and favorable flow characteristics. Additionally, particle size can be controlled by adjusting parameters such as metal flow rate, gas pressure, gas flow, and nozzle design. To prevent oxidation, inert gases such as nitrogen or argon are typically employed. Notably, approximately 95% of the carbon footprint associated with GA is attributable to

gas consumption during the atomization process [21,44]. In a study by Faludi et al. [45], the energy required for GA AlSi10 powder was found to be 8.1 MJ/kg (2.25 kWh/kg), underscoring the significant energy demands of this process. Other studies show that aluminum powder production by GA can consume up to 42 MJ/kg (11.5 kWh/kg), resulting in approximately 5 kg of CO_2 emissions per kilogram of aluminum produced [21,44]. Yields for PBF-LB/M powders are typically 20 to 40%, depending on gas die configurations, such as free-fall or close-coupled systems. Particles that fall outside the target size range are discarded, driving energy use beyond 180 MJ/kg (50 kWh/kg) and CO_2 emissions over 25 kg per kilogram of usable PBF-LB/M aluminum powder. To optimize gas consumption in the gas atomization process, Tsirlis and Michailidis [46] have developed an advanced technique employing a Venturi nozzle [47]. This method utilizes carbon dioxide to generate aluminum powder at an exceptionally low pressure of 0.5 bar. It offers a cost-effective and energy-efficient solution, while also being environmentally sustainable, thus presenting significant potential for industrial application. Plasma atomization employs plasma torches to melt metal wire, with the resulting droplets being cooled and collected in a manner similar to gas atomization. This process is inherently more energy-intensive than gas atomization due to the high temperatures required to sustain the plasma arc. In contrast, centrifugal atomization involves the rapid spinning of molten metal to generate powder particles. This technique is primarily utilized in specialized industrial applications, particularly for lower-melting-point alloys, where concerns such as erosion of the spinning disk or cup are less pronounced. Centrifugal atomization is characterized by lower energy consumption, primarily due to its reduced reliance on energy-intensive inert gases, making it a more energy-efficient alternative [48–50].

In order to offer potential solutions to the environmental and economic limitations of traditional approaches, alternative techniques to produce metal powder for additive applications have been specifically developed. These innovative methods, though less commonly utilized, have been developed with a focus on minimizing energy consumption, reducing material waste, and optimizing overall resource efficiency, making them promising candidates for addressing the environmental and economic challenges associated with traditional approaches. The Cold Mechanically Derived (CMD) process has been developed as an energy-efficient, solid-state approach that enables local, on-demand production of AM feedstock. Metal Powder Works' DirectPowder™ process offers a sustainable alternative to traditional metal powder production by employing mechanical forces to convert feedstock into fine powder particles without the need for high-temperature atomization. This low-energy approach incorporates methods such as crushing, milling, and grinding, enabling efficient conversion of raw materials to powder with a 95% yield rate while conserving energy. By eliminating the energy-intensive melting stage, CMD can reduce CO_2 emissions by up to 90% compared to conventional atomization processes [51]. CMD powders are typically irregular and non-spherical in shape, which may affect flowability and packing density in specific AM applications. However, in a study by Martin et al. [44], CMD powder was evaluated against conventional GA powder for Al7075 alloy. The results indicated that CMD powder is capable of achieving material properties comparable to those of wrought materials. Despite its non-spherical morphology, CMD powder demonstrated effective performance in PBF-LB/M applications, establishing it as a viable alternative to GA powder. Key benefits include reduced energy consumption and improved material availability, highlighting its potential for sustainable manufacturing solutions. Another effective approach to enhance the sustainability of powder production is spheroidization, a cutting-edge technique that outperforms traditional methods. Plasma spheroidization technology produces highly spherical particles with greater efficiency, improved performance, and reduced impurities, making it an ideal choice for modern manufacturing. In this process, high tem-

peratures generated by plasma melt powder particles, causing surface tension to reshape them into spherical forms as they descend through the reactor chamber. This method is versatile, capable of spheroidizing a wide array of materials, and is particularly well-suited for diverse industrial applications [52]. The UniMelt® process developed by 6 K exemplifies this advanced spheroidization technology. Utilizing microwave-based plasma, it eliminates the need for high-velocity gases, significantly reducing the risk of gas entrapment and ensuring the production of highly dense, spherical particles. UniMelt® provides precise control over particle size distribution (PSD), resulting in yields close to 100% within the desired PSD range. Tailored for AM processes such as powder bed fusion, this technique optimizes powder flowability and density, thereby enhancing overall performance. In addition to its technical benefits, the UniMelt® process is highly sustainable. It converts feedstocks such as used powders, swarf, and scrap metal into high-value metal products. By offering competitive rates for clean scrap metal, it promotes recycling and supports the economic viability of sustainable manufacturing. Furthermore, the UniMelt® process is exceptionally energy-efficient, consuming 92% less energy and generating 91% fewer carbon emissions compared to traditional manufacturing methods, while transforming waste materials into valuable metal powders [53]. Table 1 provides a comparative overview of various metal powder production methods for PBF-LB/M, highlighting their equipment costs, key features, advantages, and limitations.

Table 1. Overview of metal powder production techniques with key process details, feedstock types, particle shapes, and equipment costs.

Technique	Process	Energy Source	Feedstock	Particles Shape	Equipment Cost
Atomization	Water atomization	Induction heating	Scrap or ingot	Irregular	Low to Medium
	Gas atomization	Induction heating	Scrap or ingot	Spherical	Medium to High
	Centrifugal atomization	Induction heating	Scrap or ingot	Spherical to slightly irregular (semi-spherical)	Medium
	Ultrasonic atomization (rePowder)	Induction heating/Plasma	Any form	Highly spherical	Medium
	Plasma atomization	Plasma	Wire	Highly spherical	High
Spheroidization	Plasma spheroidization	Plasma	Irregularly shaped powder particles	Highly spherical	High
	Microwave-Based Plasma (UniMelt)	Plasma	Any form	Highly spherical	High
Mechanical	Cold mechanically derived (Direct powder)	Mechanical work	Metal rod	Irregular	Medium

3.2. Powder Obtained by Secondary Raw Material

Given that mining and primary production are the primary sources of energy consumption in AM using PBF-LB/M technology [33,54], the use of secondary materials as raw input for powder production has become a critical focus of both academic and industrial

research. Conventional alloy feedstocks used for metal powder production entail substantial energy consumption and significant carbon emissions throughout the production chain. This challenge encompasses global logistics, including transportation, melting, and forming of materials into billets, bars, coils, or wire feedstock, and extends to the energy-intensive refinement of ores into elemental metals, a process that heavily depletes natural resources. Relying solely on virgin raw materials for powder production not only drives up costs but also amplifies environmental impacts, particularly as demand for metal powders continues to rise.

Contrary to the common misconception that all metal powders are derived from virgin primary metal stocks, the industry has evolved significantly in recent years. It is now widely recognized that some metal powders are produced from recycled secondary feedstock. The economic advantages of utilizing qualified scrap over virgin raw materials are considerable, largely due to the reduced energy requirements. Substituting virgin raw materials with scrap feedstock can significantly lower CO_2 emissions, with reductions of several kilograms of CO_2 per kilogram of alloy produced. The primary challenge moving forward is ensuring that scrap materials meet the necessary size and chemical composition specifications.

Aluminum alloys can be engineered for enhanced recyclability without a significant loss in properties. This increased recyclability decreases the need for raw material extraction and processing, thereby minimizing the overall environmental impact. Continuum's advanced technology leverages only secondary metal materials to produce high-quality AM-grade powder, achieving up to an 80% reduction in carbon emissions compared to conventional metal recycling methods [55]. The powder is sourced entirely from recycled metals and is manufactured using 100% renewable energy and upcycled, purified argon gases. rePowder, developed by Amazemet, is an advanced research platform that leverages patented ultrasonic technology to produce high-quality AM-grade powders from a wide range of alloy systems [56]. This system generates powders with a narrow particle size distribution, with up to 80% of the output ready for immediate processing. Equipped with both arc/plasma and induction melting modules, rePowder can handle a variety of melting temperatures, making it versatile for different materials. It efficiently atomizes raw materials, scrap, and failed printouts into spherical powder particles, offering a sustainable solution for prototyping new alloys and recycling rare or valuable materials.

Thanks to recent advancements in engineered methods, it is now possible to produce high-quality powders with the shape and PSD required for AM technologies like PBF-LB/M. However, a critical challenge that remains unresolved is the issue of contamination in aluminum alloys derived from secondary raw materials. Contaminants can significantly impact the mechanical properties, processability, and overall performance of the final components, raising concerns about their suitability for demanding applications. An example of unwanted contamination is the presence of iron traces in recycled Al-Si alloys. Iron contamination exceeding 0.5 wt% is almost universally discouraged, as it leads to the formation of undesirable phases, including the brittle Al5FeSi (β) phase, which significantly compromises the ductility and mechanical performance of the material [57]. Since a reliable and economical method for removing iron from Al-Si alloys does not exist in metallurgical practice, the literature has turned to the exploration of iron correctors such as Mn, Ni, Co, Cr, Ti, V, and Mo [58]. In order to obtain the Al-Fe-Si-Cr-Ni compositions considering the pivotal aspect of sustainability, Bhatt et al. decided to start from ingots of two of the most widespread alloys for AM and conventional processes: AlSi10Mg (for Al and Si elements) and AISI 304L (for Fe, Ni, and Cr elements) [59]. This approach involves blending commercially available alloys in precise proportions instead of synthesizing new compositions from pure elements. It promotes sustainability by enabling the use of recycled alloys, reducing the environmental impact of powder production, and simplifying alloy

qualification. Metallurgically, mixing established alloys allows control over microstructural evolution, leveraging known phase diagrams and solubility limits. This facilitates the optimization of strengthening mechanisms, such as precipitation hardening and grain refinement, while minimizing trial-and-error in alloy design. Additionally, strategic alloy blending helps mitigate impurity-related issues in secondary raw materials, improving overall material performance.

3.3. Powder Reuse

Sustainability in metal powder usage extends beyond incorporating recycled feedstock; it also encompasses the recycling and repurposing of powders that have undergone AM processes. Due to the layer-by-layer nature of the PBF-LB/M process, a considerable amount of metal powder surrounding the solidified part remains unused. To maximize material efficiency and minimize waste, these powders must be reclaimed and reused in subsequent builds. A comprehensive understanding of this aspect of sustainability is essential to fully grasp how powder recycling contributes to the circular economy.

Powder particles near the melt pool, but not fully incorporated into the part, as well as those that remain on the building plate or are carried into the overflow tank, can experience varying levels of heat exposure during the build process [60]. This differential exposure can lead to distinct effects on the particles, influencing their shape and flowability. Heat exposure can cause agglomeration or sintering, resulting in larger particles with satellites and increased surface roughness [61]. Furthermore, spattered particles from the melt pool can create agglomerates and oxides in the surrounding powder bed [62]. Although sieving is commonly used to remove larger particles, particle shape and surface chemistry alterations can still influence powder flowability, packing, and, consequently, the quality of the powder bed. A poor-quality powder bed can, in turn, impact the densification of the component produced through PBF-LB/M, and thus its mechanical properties, as observable in Figure 5.

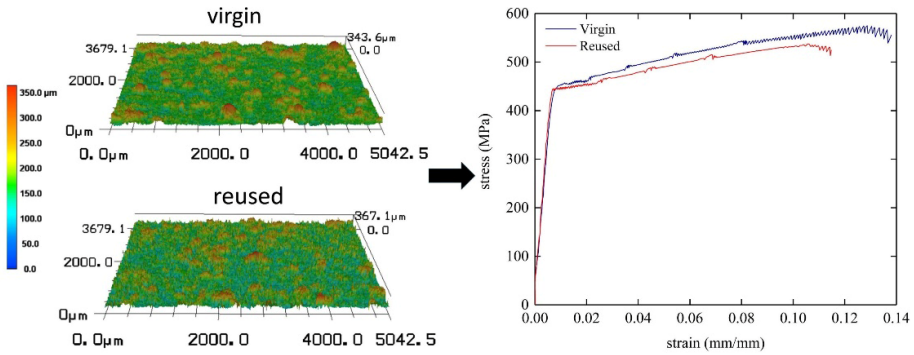

Figure 5. Surface morphology and mechanical behavior comparison between virgin and reused powder in PBF-LB/M of Al–Mg–Sc–Zr alloy [63].

ASTM F3318-18 [64], which pertains to AlSi10Mg, and ASTM F3592-23 [60], which provides guidelines for feedstock reuse, both permit the recycling of previously used powder. After each build cycle, the remaining powder may be blended with virgin powder to maintain sufficient quantities for subsequent builds. To ensure compliance with quality standards, regular chemical analysis of the recycled powder is required. Additionally, all the used powder must be sieved using a mesh with appropriate sizing to effectively remove agglomerates and contaminants from the build process. Asgari et al. [65] investigated the use of recycled AlSi10Mg powder in PBF-LB/M, comparing the properties of virgin powder, heat-affected condensate particles, and recycled powder. The study revealed that recycled powder exhibited characteristics similar to those of virgin powder, confirming

its suitability for use in PBF-LB/M without compromising the quality of the final product. Cordova et al. [63] investigate the impact of powder reuse on the properties of Al–Mg–Sc–Zr alloy (Scalmalloy®), focusing on key characteristics such as morphology, composition, and particle size distribution in both virgin and reused powders. The study also evaluates the mechanical properties of specimens produced from virgin powder and those after four build cycles, assessing the effects of blending reused and virgin powder on the final material properties. Although the microstructure of the specimens remains largely consistent, the reused powder introduces slightly higher porosity, characterized by small micro-sized pores; however, these do not significantly influence the mechanical properties. The findings indicate that Al–Mg–Sc–Zr powder can be effectively reused for up to four build cycles, provided proper sieving is applied and 40% of the powder is refreshed with virgin material. Another study by Smolina et al. [66] evaluated the reuse of AlSi7Mg0.6 powder in the PBF-LB/M process. The findings showed that the powder could be reused up to five times with minimal degradation, supporting its viability for sustainable and cost-effective manufacturing.

Studies on the effect of powder recycling on the quality of aluminum parts produced by PBF-LB/M are numerous, yet often contradictory when it comes to determining the optimal proportion of recycled powder to virgin powder and the analytical techniques needed to assess the suitability of recycled powders. These discrepancies arise from the complexity of the AM process, the variability introduced by the diverse aluminum alloys used, and how their chemical composition can make them more or less susceptible to undesirable phenomena such as surface oxidation. Furthermore, numerous factors prevent the establishment of a universal standard for the number of reuse cycles, after which a powder is still considered viable for PBF-LB/M processing. This limitation stems not only from the specific material used but also from process conditions and prior build characteristics. For instance, the geometry of previously manufactured parts plays a crucial role in powder degradation. The greater the volume occupied by massive components, the larger the surface area in contact with the surrounding powder bed. Consequently, this increased interaction likely accelerates powder degradation, affecting a more significant fraction of the reused material. To the best of the authors knowledge, no studies have systematically investigated this aspect, yet it presents an intriguing opportunity for future research to refine powder reuse strategies and enhance the additive process sustainability. Another aspect that is rarely mentioned in the literature is how the reused powder is sampled for different studies. Understanding the sampling methodology could provide valuable insights into the inconsistencies observed across various works and help standardize evaluation criteria.

4. PBF-LB/M Process

4.1. Design

In recent decades, several industrial sectors have undertaken initiatives to reduce fuel consumption and greenhouse gas emissions. One promising solution is lightweighting through material substitution and component redesign [32]. In the automotive industry, the need to lighten vehicle components is closely related to the aim of minimizing fuel consumption for economic savings and environmental sustainability. Lighter vehicle components decrease the inertial forces that the engines must overcome, resulting in lower fuel consumption. Electrically powered vehicles also benefit from lightweighting, as it reduces the need for heavier and more expensive batteries to maintain driving ranges [67]. In addition to replacing traditional materials with lightweight high-performance alloys, redesign can be used to lighten components. In this research context, AM emerged as a disruptive potential substitute for traditional manufacturing processes. It offers greater design freedom, higher capability for mass customization, and the ability to produce

complex structures while minimizing waste streams. The adoption of AM offers significant energy-saving potential also in aviation, potentially reducing airplane fuel consumption by up to 6.4% and enabling substantial secondary weight savings through new design methods [68]. Among AM technologies, PBF-LB/M offers cost-effectiveness when dealing with high geometric complexity and low production quantities. These benefits, combined with materials engineered for the process that provide desired properties and quality, contribute significantly to sustainable development in metal AM [69,70].

4.1.1. Novel Lightweight Compositions

To enhance sustainability and efficiency, the design of novel high-performance, lightweight alloys explicitly tailored for the PBF-LB/M process is crucial. These lightweight alloys, with optimized strength-to-weight ratios, are essential for advancing sustainability by reducing material usage and improving overall component performance. By developing alloys with a high strength-to-weight ratio, it is possible to ensure the suitability for components that require excellent mechanical properties while remaining light, which is crucial for fuel-dependent industries [71]. Integrating novel lightweight materials in the automotive sector has shown substantial promise, achieving total weight reductions of 20–45% in innovative vehicle designs. Notably, weight reductions of 20–35% have been linked to fuel consumption decreases of 12–20%, underscoring the critical importance of material advancements in driving sustainable and energy-efficient automotive innovation [72]. Lightweight aluminum alloys often replaced traditional steel and iron components, yielding a weight savings of 40–60% with a cost premium of 1.3–2 [73]. Constituting about 9% of an average vehicle mass [72], aluminum is widely employed in components such as engines (e.g., housing), wheels, and transmissions due to its excellent strength-to-weight ratio, enabling 1 kg of aluminum to replace 2–4 kg of steel. Aluminum alloys play a critical role also in aerospace structures, valued for their lightweight properties and extensively utilized in components such as fuselage skins, upper and lower wing panels, and wing stringers [74]. Innovative aircraft designs are critical for advancing the efficiency and sustainability of modern air travel. Reducing structural weight enables aircraft to carry greater payloads, whether passengers or cargo, without increasing fuel consumption. This optimization translates into lower operational costs, more efficient route planning, and substantially reduced carbon emissions. Notably, a 1% reduction in aircraft weight typically results in an approximate 0.75% decrease in fuel consumption, underscoring the importance of lightweight strategies [75]. The Boeing 787 is a benchmark in leveraging advanced lightweight materials, achieving a 20% weight reduction compared to similar aircraft. This innovation delivers fuel efficiency gains of 10–12%, demonstrating the transformative potential of material advancements in achieving more sustainable aviation practices [76].

High-performance aluminum alloys can provide the mechanical and thermal properties required for specific applications while achieving weight reduction goals. Typical commercial aluminum alloys used in the automotive and aerospace industries are low-cost, age-hardenable wrought aluminum alloys, such as the 2xxx and 7xxx series, which have good mechanical properties and can meet a wide range of industrial requirements. However, these alloys are characterized by poor processability due to their high susceptibility to hot cracking caused by rapid melting and solidification [77]. Consequently, the number of these alloys that can be successfully processed using PBF-LB/M and other fusion-based AM processes is quite limited. Currently, the aluminum alloys that can be additively manufactured with lasers are mainly near-eutectic Al-Si-based alloys [78]. This is due to their short solidification range (the temperature range between liquidus and solidus for a material with a distinct chemical composition during which solidification occurs) and consequently their low susceptibility to hot cracking [11]. Although quasi-eutectic

compositions have shown good manufacturability, they fail to meet industrial requirements in terms of mechanical properties and high-temperature performance. Therefore, research into novel, high-performance aluminum alloys compatible with the PBF-LB/M process is continually progressing. The objective is to attain the necessary mechanical and thermal properties for demanding applications, achieve weight reduction goals, and minimize issues like cracking and solidification defects.

In the literature, proposed solutions to address hot cracking include changing the chemical composition to narrow the solidification range and refine the grain structure or modifying alloy solidification conditions reducing the heat flow and the cooling rate by optimizing the process parameters [79]. Finding the optimal process parameter combinations requires extensive studies involving non-cost-effective and time-consuming experiments through a trial-and-error approach. In addition, while optimizing process variables has shown effectiveness in reducing component internal defects, resulting in an improvement of the quality and uniformity of printed parts, this approach has generally failed to completely eliminate hot cracking phenomena in the toughest alloys [80]. This implies that hot cracks can still occur even under the best process conditions. To enhance printability and avoid detrimental hot cracks, it is essential to either develop new alloys or modify existing compositions [81].

Fine equiaxed microstructures proved to exhibit greater capacity to accommodate strain in the semi-solid state [77]. Furthermore, fine grains facilitate efficient liquid feeding and the healing of initial cracks, enhancing their resistance to hot cracking. Additionally, due to their increased grain boundary area within the material bulk, finer grains suppress the accumulation of low-melting elements or phases at grain boundaries. Considering the high hot crack sensitivity of different aluminum alloys, much research has concentrated on studying compositional variations that can result in grain refinement preventing hot cracks [82]. For instance, Martin et al. [77] demonstrated that adding 1 vol% ZrH_2 nanoparticles as nucleation agents in Al-Zn and Al-Si-Mg alloys significantly refined the microstructure by enhancing heterogeneous nucleation and promoting equiaxed grain growth. This method successfully eliminated hot cracking in both Al7075 and Al6061 alloys processed by PBF-LB/M. On the same research line, different studies investigated the impact of incorporating various elements or compounds (including Ti, Zr, Sc, Er, Si, and different compounds such as oxides like TiO_2, carbides like TiC and borides like CaB_6 and TiB_2, as well as carbon allotropes like graphene and carbon nanotubes) on refining the grain structure and so on reducing hot cracking in high-strength Al-based alloys [83]. For example, a study conducted by Li et al. revealed that adding a Ti/TiN hybrid grain refiner into the PBFed 7050 alloy leads to the formation of ultrafine grains [84]. The approach involves either promoting heterogeneous nucleation or introducing solutes with a high growth restriction factor to rapidly provide sufficient constitutional supercooling for nucleation at the front of the solid-liquid interface.

Adjustment to alloy compositions, such as adding grain refiners to promote the heterogeneous nucleation of Al grains, is not merely an academic approach but is increasingly used in industrial fields as well [82]. One of the leading U.S. manufacturers of metal powders, Elementum 3D, features in its portfolio of Al-based compositions enhanced versions of traditional alloys and advanced dispersion-strengthened aluminum powders for PBF-LB/M production formed by a process called reactive additive manufacturing (RAM). The RAM process enables the formation of advanced metal matrix composites that combine a continuous metal matrix with high-strength reinforcing ceramic or intermetallic phases. This approach allows printing materials with unique and advantageous combinations of ductility, strength, toughness, stiffness, fatigue resistance, and high-temperature performance. Following this approach, the Elementum 3D metal powder portfolio includes

modified compositions such as Al6061+RAM and Al7050+RAM, in which ceramic nanoparticles like TiB_2, Zr, and TiC are incorporated into the Al-based traditional alloys to improve printability [85].

In addition to modifications to traditional compositions, another approach that can be undertaken to improve processability for PBF-LB/M without incurring hot cracking and other detrimental phenomena while improving the material performance in extreme conditions is the formulation of tailored compositions. Among the Al-based compositions specifically developed for the PBF-LB/M process, the patented Scalmalloy (an Al-Mg-Sc alloy) and A20X (an Al-Cu-Ti alloy) stand out. Scalmalloy, developed by APWORKS, is a high-performance alloy that combines exceptional strength, ductility, and corrosion resistance with low density, making it ideally suited for aerospace, automotive, and other sectors where weight reduction and structural integrity are critical [86]. Sc has a significant impact on the properties of aluminum alloys through its effectiveness as an inoculant, which enhances the formation of fine-grain structures [87]. Additionally, it forms a limited-solubility eutectic diagram with aluminum. Upon cooling, the high-temperature Al-Sc solid solution can decompose, generating finely dispersed and fully coherent Al_3Sc intermetallic precipitates. These precipitates are notably effective in inhibiting recrystallization, even at elevated temperatures [88]. In addition, Scalmalloy ultrafine and nanoscale microstructure proved to result in exceptional strength and ductility, as well as impressive fatigue resistance [89]. The A20X alloy, developed by Aeromet International, is an advanced aluminum–copper (Al-Cu) alloy system enhanced with TiB_2 nanoparticles for grain refinement. Initially engineered for casting applications, A20X has demonstrated exceptional mechanical properties, including superior strength and fatigue resistance. In response to the increasing demand for high-strength, lightweight materials in the aerospace and defense sectors, Aeromet successfully optimized A20X for PBF-LB/M, enabling the production of complex, high-performance components [90].

Recently, Constellium launched Aheadd®, a new generation of high-performance aluminum powders designed for the PBF-LB/M process. Among these, Aheadd® CP1 is ideal for high-conductivity applications, while Aheadd® HT1 is perfect for high-temperature applications [91]. CP1 is an innovative Al-Fe-Zr alloy that exhibits excellent processability, high yield strength, and improved thermal conductivity following direct aging. The formation of primary Al3Zr prevents hot cracking, while direct aging induces the dual precipitation of coherent nano-Al3Zr and plate-like Al13Fe4, boosting the yield strength. Furthermore, the reduction of the supersaturated matrix achieved through PBF-LB/M leads to a simultaneous increase in conductivity [92,93]. Aheadd® HT1 is an Al-Mn-Ni-Cu-Zr alloy specifically engineered for PBF-LB/M applications requiring high strength and service temperatures up to approximately 260 °C. Its excellent thermal stability makes Aheadd® HT1 an ideal substitute for AA2xxx aluminum-copper high-temperature alloys. Additionally, it opens up new design opportunities by leveraging aluminum high thermal conductivity and low density, allowing it to be used in service conditions that traditionally require titanium or steel [91]. Table 2 shows some examples of aluminum alloys suitable for PBF-LB/M.

Table 2. Aluminum powders suitable for PBF-LB/M technique.

	Name	References
Traditional alloys	AlSi10Mg	[94]
	AlSi7Mg	[95]
	AlSi12	[96]
	Al6061	[97]
Modified alloys	A1000-RAM10	[85]
	A6061-RAM2	[85]
	A7050-RAM2	[85]
	Al2024 + Y element	[98]
	Al7075 + Si element	[99]
	Al7075 + ZrH_2 elements	[77]
	Al6061 + ZrH_2 elements	[77]
	AlMgty	[100]
	AlZnty	[100]
Tailored alloys	Al8Ce10Mg	[80]
	Al-Fe-Zr (CP1)	[92]
	Al-Mn-Ni-Cu-Zr (HT1)	[91]
	Al–Mg–Li–Ag-Sc-Zr	[101]
	AlZnMgScZr	[102]
	Al58Zn28Mg6Si8	[103]
	Al-mg-Sc (Scalmalloy)	[88]
	Al-Ni-Cu	[104]
	Al-Cu-Ag-Mg (A20X)	[90]

4.1.2. Structural Optimization

The growing focus on sustainable transportation and the quest for higher efficiency, specifically through reduced energy consumption, has spurred research efforts to develop lightweight and strong designs. Reducing vehicle weight is a pivotal strategy for decreasing petroleum consumption and greenhouse gas emissions. Studies indicate that a 100 kg reduction in vehicle weight can lower fuel consumption by approximately 0.69 l/100 km [72] and lead to a decrease of 6 g/km in CO_2 emissions. Each kilogram of weight reduction contributes to a total reduction of approximately 20 kg of CO_2 emissions over a vehicle operational lifespan [105]. Two main strategies for achieving lighter structures have emerged: topology optimization (TO) and latticing. TO is a method of optimizing shapes by algorithmically adjusting material distribution within a specified space to meet prescribed loads, conditions, and constraints. The most prominent TO approaches can be summarized as follows: density-based; level set; evolutionary; topological derivatives; and phase field and homogenization [106–108].

Density-based TO is widely used in academia and generally follows a standard procedure. This approach is structured using the finite element method [109] where each element density is a design variable, allowing for an optimal layout of element distribution within the designated design area. In density-based TO, elements are assigned density values ranging from 0 to 1, where 0 signifies a void, 1 signifies a solid, and values between 0 and 1 indicate intermediate densities. To enforce a discrete combination of solid and

void regions, density-based TO leverages the Solid Isotropic Material Penalization (SIMP) method, which penalizes intermediate-density elements. The SIMP method addresses a minimization problem typically involving the volume fraction of the design space or structural compliance (C). The goal is to maximize the stiffness of the structure, which can be evaluated over the entire domain or within the designated design space. Various constraints, such as mass, load, or displacement limits, can be applied, and customized objective functions with weighted criteria can be incorporated. Furthermore, TO can be adapted to include manufacturing constraints, ensuring that the resulting designs are feasible for fabrication [110]. The general formulation of the SIMP method for the compliance minimization problem is as Equation (1) [111,112]:

$$Minimize\ C = \frac{1}{2}\sum_{i=1}^{L} f_i u_i^T = \frac{1}{2}\sum_{i=1}^{L} f_i^2 \left((\rho_i)^P k_0\right)^{-1} \quad (1)$$

In this equation, "C" represents compliance, "f" is the external load vector, "u" is the global displacement vector, and "L" is the total number of finite elements. "ρ_i" is the density of the ith element, and the parameter "P" denotes the penalization factor, with a range of $1 < P \leq 3$. "k_0" signifies the stiffness of the ith element before penalization.

Components designed through TO often include free forms and intricate shapes that are complex or impossible to manufacture with traditional production methods. However, these designs are ideally suited to the PBF-LB/M process, which offers more flexibility in design rules and can efficiently reproduce complex geometries without incurring additional costs [113,114]. The advantages of combining topology optimization with AM technology can be categorized into saving both money and time by using reduced material and avoiding additional costs. By reducing the weight, the TO can lower fuel consumption and emissions, increase payload and range, and enhance the maneuverability and agility of the aerospace or mobility industry [115]. However, the practical adoption of these optimized designs depends not only on their performance benefits but also on the ability to manufacture them efficiently and cost-effectively. The complexity of topology-optimized and lattice structures can pose challenges in production, particularly in ensuring dimensional accuracy, minimizing defects, and achieving consistent mechanical properties. Process parameters, material selection, and advanced post-processing techniques play a crucial role in overcoming these hurdles.

While the initial design phase, computational simulations, and extended production times may lead to higher upfront costs, these can be offset by long-term benefits such as material savings, improved efficiency, and enhanced performance throughout the component lifecycle. In fact, this approach aids in overcoming design challenges, particularly in creating lightweight components for many industrial fields such as automotive and aerospace. Several case studies on the TO of aerospace components, such as the connector support of the VEGA space launcher, a typical lever component from civil aircraft, a housing part from fan cowl structures, and a jet engine bracket, demonstrate mass reductions ranging from 20 to 60% [116,117]. Also, several case studies on the topology optimization of automotive components have shown significant improvements. For example, brake calipers achieved a 41.6% mass reduction, the steering upright became 9% lighter than the reference component, and the optimized automotive knuckle part exhibited a stiffness increase of more than 2.5 times compared to the original design [118–120]. Furthermore, this approach is particularly appreciated when combined with the use of lightweight, high-performance alloys. To cite an outstanding example, APWorks has developed the world first 3D-printed motorcycle utilizing PBF-LB/M technology and the patented Scalmalloy® material [121]. This innovative creation, illustrated in Figure 6a, known as the Light Rider, stands out as an exceptionally lightweight model, weighing just 35 kg [46]. Its 6 kW electric motor propels

it from zero to 80 km/h within seconds, demonstrating impressive acceleration. The motorcycle frame, a mere 6 kg, contributes to its remarkable 30% weight reduction compared to conventionally manufactured e-motorcycles. APWorks employed an algorithm to design the Light Rider's optimized structure, achieving a minimal weight while ensuring frame robustness to endure everyday driving demands and stresses. RUAG Space has developed an optimized antenna bracket, measuring 40 cm in length, for Sentinel satellites using PBF-LB/M with AlSi10Mg (Figure 6b). Engineers redesigned and optimized this part using Altair ProductDesign which is SIMP-based software 2023, followed by production utilizing an EOS M400 machine. By enhancing the structural design, they achieved a stiffness increase of over 30% above the minimum requirement while reducing the weight from 1.60 to 0.94 g. This improvement represents a substantial performance enhancement along with a weight reduction exceeding 40% compared to the conventionally manufactured component [122,123].

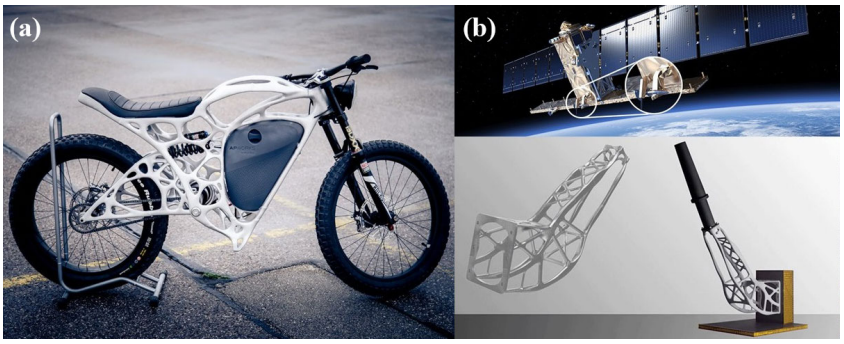

Figure 6. Examples of topology-optimized structures manufactured by PBF-LB/M: (**a**) the Light Rider, the first 3D-printed electric motorcycle by APWorks [121] and (**b**) an optimized antenna bracket for RUAG Sentinel satellites [123].

The second primary strategy for achieving lighter structures is latticing. Lattice structures are composed of repeating unit cell elements in three-dimensional space. Thanks to AM, lattices offer numerous advantages: they enhance object strength, reduce mass by using less material, lower production costs by shortening build times, decrease fuel usage through lighter component weight, and minimize material waste. To design lightweight structures with high mechanical performance, natural structures such as cork, sea urchins, honeycombs, and trabecular bone are often used as models. The three most common families of lattice structures are: surface-based lattices, strut lattices (periodic and stochastic), and planar-based lattices.

Architected materials are precisely engineered structures designed to achieve specific, controlled physical responses. This class of materials exhibits novel or customized behaviors through the interaction of their intrinsic material properties and carefully designed geometries. Lattice structures are a subset of architected materials, consisting of repeating networks of interconnected nodes and beams (or other structural elements), often optimized for mechanical performance. By utilizing lattice-based designs, these materials can precisely manipulate thermal, electromagnetic, mechanical, or biological properties. Architected materials enable fine-tuning of a component behavior by modifying its geometry at the mesoscale, such as in auxetic materials, which exhibit a negative Poisson ratio, rather than relying solely on changes to the material microstructure [124–126].

Employing lattice structures facilitates component lightweighting, effectively reducing part weight while preserving structural integrity. Latticing provides the means to decrease solid mass without compromising performance. Additionally, lattices can be fine-tuned to construct high-energy or shock-absorption structures. For instance, auxetic lattice structures, characterized by their negative Poisson ratio, exhibit excellent behavior in

energy absorption and damping. Moreover, lattice structures inherently offer a large surface area, making them ideal for heat transfer and particularly advantageous for thermal management and heat exchanger applications [127]. Figure 7 depicts various applications of lattice structures, including heat exchangers (a), orthopedic implants (b), and vibration isolation (c).

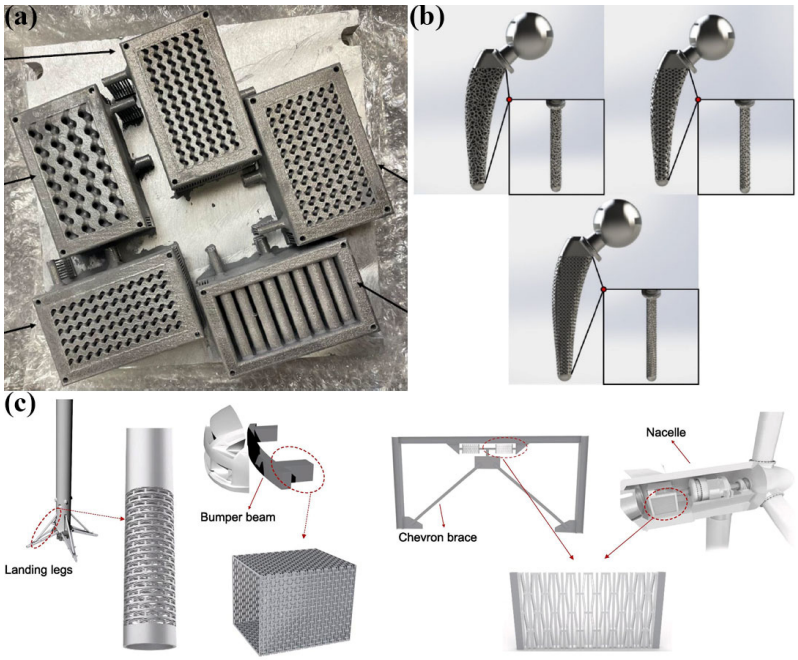

Figure 7. Some applications of lattice structures: (**a**) heat exchangers [127], (**b**) orthopedic hip implants [128], and (**c**) real-world scenarios of passive impact and vibration isolation [129].

With the synergic use of TO and latticing, the highest levels of lightweightness, and thus sustainability and efficiency, can be achieved. A case study where TO and latticing were used for the structural optimization of the VEGA space launcher connector support made of aluminum alloy Al7075 is illustrated in Figure 8 [117]. The optimized configurations resulted in a weight reduction of up to 63%. The latticing design strategy, which includes incorporating grid structures into the holes produced by the optimization process, was adopted to enhance manufacturability. In particular, grid structures were used on topology-optimized configurations, which strongly reduced the amount of support needed. This optimization also resulted in a weight reduction of connector supports by about 57% compared to the main component [117].

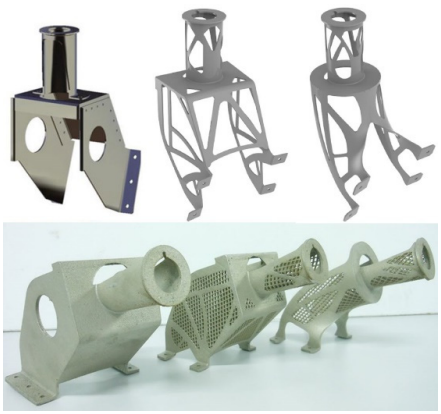

Figure 8. Case study of VEGA space launcher connector support optimization by TO and latticing [117].

4.2. Process Optimization

Reducing environmental impact, optimizing resource efficiency, and upholding economic and social responsibility are critical priorities for the AM industry. By refining PBF-LB/M process parameters, manufacturers can significantly minimize power consumption and decrease defects and rework, thereby conserving materials, energy, and time, all of which are vital for advancing sustainability. By leveraging Design of Experiments (DoE) to identify optimal process parameters, improving productivity through strategic adjustments, deploying state-of-the-art PBF-LB/M machines, and implementing rigorous monitoring and quality control to extend component lifespan, manufacturers can achieve not only superior environmental performance but also significant economic and operational benefits. These advancements reinforce PBF-LB/M as a more sustainable and viable manufacturing technology in the long term.

4.2.1. Novel Time-Save Approach for the Design of Experiments

The PBF-LB/M process is influenced by over 50 parameters, including laser characteristics (such as the type of laser source, laser energy, scan speed, spot diameter, and focus position) and scan strategies (including hatch pattern and rotation, beam compensation, and the sequence of hatch/contour scans) [69,130]. This large number of process parameters makes control and quality assurance challenging and time-consuming. Additionally, each parameter set must be specifically tailored to the powder and machine being used, further complicating the optimization process [131].

One approach widely used for scientific experimentation in traditional processes is the One-Variable-At-a-Time (OVAT) method, where one variable is altered while all others are kept constant to assess each variable effect independently. Once the optimal value for a variable is identified, it is set, and the next variables are examined similarly. However, this approach has significant drawbacks. As proved by Benedetti et al., the OVAT method is unsuitable for experiments involving numerous factors and fails to effectively observe the interactions between interconnected factors [132]. Given the complexity of PBF-LB/M, analyzing OVAT is impractical due to the vast number of tests required.

DoE methodologies provide a more efficient approach to optimizing process parameters, particularly when the relationships between parameters and outcomes are poorly understood. This lack of understanding can hinder the development of effective control methods. Applying DoE can quantify the correlations between parameters and process outcomes, which is crucial for improving PBF-LB/M results. Through parameter optimization, DoE can reduce surface roughness, enhance mechanical properties, and lower defect rates, ultimately increasing sustainability by extending the lifespan of components. DoE also minimizes material waste and reduces energy consumption, resulting in more efficient production at lower costs. Additionally, it fosters a deeper understanding of process interactions, encourages the use of sustainable materials, and promotes innovation in AM [133,134].

To carry out a DoE, the following six steps should be followed [135–137]:

- Planning: Clearly define the experiment objective and scope to ensure a specific purpose and avoid the common error of conducting experiments without a clear aim.
- Screening: Identify all potential factors that could influence the outcome. This step involves selecting key variables and avoiding the mistake of "sentimental screening" based on personal biases rather than scientific evidence. Screening methods include full factorial, fractional factorial, and Plackett–Burman designs.
- Modelling: Design the experiments by choosing relevant factors, determining their ranges, and selecting an appropriate experimental design (e.g., factorial, response surface methodology). This step includes creating a plan to vary the factors systematically.

- Execution: Perform the experiments according to the designed plan, ensuring accurate and consistent data collection. This step is crucial for gathering data and model development and optimization.
- Analysis and Optimization: Analyze the experimental data using statistical methods to develop a model that describes the relationship between factors and responses. Use this model to identify optimal conditions and validate the results through confirmation runs. Optimization techniques include response surface methodology designs such as Central Composite Design and Box–Behnken Design, as well as mixture designs like simplex centroid design and simplex lattice design.
- Verification and Validation: Confirm the experimental findings by conducting additional tests to ensure the results are reliable and can be generalized. Analyze the results to convert data into valuable information and draw conclusions.

A review of the literature reveals useful applications of DoE in optimizing the processes of additively manufactured aluminum alloys [138–141]. Majeed et al. [138,139] conducted two studies focusing on optimizing processing parameters and evaluating heat treatment effects on the surface quality and relative density of PBFed AlSi10Mg alloy. They employed a three-factor, three-level full factorial DoE for both studies. In the first study, they investigated the influence of processing parameters and various heat treatment conditions on relative density, achieving maximum densification exceeding 99% under optimal conditions of 320 W laser power, 900 mm/s scanning speed, and a 25% overlap rate. In the second study, they focused on optimizing processing parameters to achieve the best surface quality. Their findings, supported by analysis of variance (ANOVA) and regression analysis, revealed that higher laser power increased surface roughness while scanning speed initially decreased roughness but showed a slight increase at higher speeds. Leal et al. [140] highlight the application of the Taguchi experiment design method to optimize the PBF-LB/M process for the AlSi10Mg alloy. By employing ANOVA, the most significant factors influencing the process were identified, with laser power being the most critical parameter affecting relative density. A regression analysis provided a linear regression equation for the model, enabling the prediction of optimal processing parameters. Maamoun et al. [141] investigate the impact of PBF-LB/M process parameters on the quality of AlSi10Mg and Al6061 aluminum alloys using a full factorial DoE. Key findings include that optimal energy densities for AlSi10Mg (50–60 J/mm^3) and Al6061 (102.8 J/mm^3) significantly influence relative density, porosity, surface roughness, and dimensional accuracy. AlSi10Mg achieved a maximum relative density of 99.7%, while Al6061 reached 98.7%. Surface roughness decreased with increasing energy density, and dimensional accuracy varied accordingly.

Despite being an efficient method to quickly define optimal process parameters for PBF-LB/M production, the DoE approach still requires producing and analyzing a significant number of bulk samples. This process demands a substantial amount of time, as well as high levels of powder and energy consumption. Several alternative techniques have emerged in recent years to accelerate parameter optimization while minimizing powder usage, time, and costs, among which the SST approach stands out. This approach is widely adopted in research and involves scanning a laser track on a single powder layer spread onto a substrate. This approach is based on the idea that PBFed parts are made of overlapping SSTs, therefore, the part properties strongly depend on the geometry of each SST and the interaction among them. Unlike massive sample production, SST scanning requires only a minimal amount of powder and a few fractions of a second as scanning time [142–145]. In the SST approach, only laser power and scanning speed are varied while the layer thickness is kept constant. This approach allows for extensive exploration of power–speed combinations due to the rapid production and analysis capabilities. By evaluating the width and continuity of the SSTs from a top view, as well as their cross-

sectional morphologies, a narrower range of power–speed combinations suitable for bulk production can be swiftly identified. To evaluate the SST quality, the widely used method is the cross-section analysis. In Aversa et al. [142] the geometrical characteristics of the SST cross-section, including the width, growth, depth, and contact angles, were examined to investigate the material melting and consolidation behavior, thus determining its suitability for PBF-LB/M production. However, the SST cross-sectional analysis involves a complex and time-consuming sample preparation procedure, and operator error could strongly affect the manual on-top evaluation. To overcome these issues, Martucci et al. [143] explored a computer-aided approach involving automated analysis to characterize SSTs. In particular, they developed a novel algorithm to filter out non-continuous scans and evaluated SST quality using three regularity indexes. Although this method has significantly speeded up the analysis of SSTs and markedly increased the reliability of obtainable results, a DOE of bulk samples, albeit a very limited one, for complete optimization is still required. Gheysen et al. and Bosio et al. [145,146] further streamlined the procedure by developing a method to derive the optimal hatch distance value directly from SSTs. Specifically, the optimal hatch distance value can be determined by calculating the width of the SSTs and ensuring adequate overlap among them. This overlap can be fixed at 0%, as recommended by Bosio et al. [145], or calculated using certain geometrical parameters of the SSTs with the equation developed by Gheysen et al. [146].

4.2.2. Strategies to Improve Productivity

One of the main challenges in AM technologies is their relatively low build rate, which makes the production rate unsuitable for efficient mass production compared to traditional manufacturing methods. For instance, while PBF-LB/M systems deposit material at rates of only hundreds of grams per hour, other methods achieve deposition rates measured in kilograms per hour, and processes like forming, stamping, and casting reach rates of hundreds of kilograms per hour [147]. To enable widespread industrial adoption, PBF-LB/M must develop a scalable architecture that significantly increases deposition rates by several orders of magnitude while still preserving the geometric flexibility inherent in AM [148]. In the PBF-LB/M process, sustainability and productivity are closely interconnected. As a result, understanding the factors that influence component production time is crucial for identifying solutions that improve both the industrial scalability of PBF-LB/M and its environmental impact. Recently, Kasprowicz et al. summarised the complexities of the PBF-LB/M process, highlighting the various factors affecting production time in the Ishikawa diagram shown in Figure 9 [149].

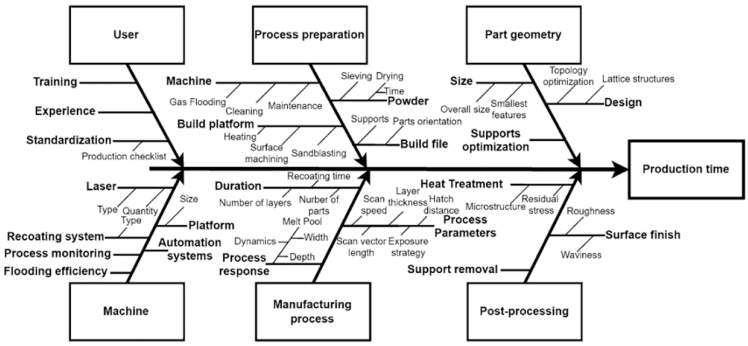

Figure 9. Ishikawa diagram illustrating the factors that impact production time in the PBF-LB/M process [149].

Methods for enhancing productivity in the PBF-LB/M process can be grouped into several areas, including adjusting process parameters, utilizing advanced equipment (such as multiple laser systems or polar coordinate setups), and adopting hybrid production systems.

One of the most widespread approaches to speed up PBF-LB/M productivity is by selecting optimal combinations of process parameters to maximize the build rate. Tang et al. [150] defined the Build Rate as Equation (2):

$$BR\ (\mathrm{cm}^3/\mathrm{h}) = hd \times l \times v \quad (2)$$

where v is the laser speed, hd is the hatch distance, and l is the layer thickness. Based on this equation, it is clear that increasing the scan speed, hatch distance, and layer thickness can significantly enhance both the productivity and sustainability of the PBF-LB/M process. However, increased v, hd, and l also result in reduced energy density, which can lead to lower-density products, with the occurrence of a lack of fusion porosities. To avoid the presence of defects that could have a detrimental effect on mechanical properties, it is, therefore, essential to balance productivity with part quality [151,152].

Defanti et al. focused on enhancing PBF-LB/M efficiency in AlSi10Mg components while maintaining high-quality standards. Their investigation into process parameters found an optimal balance between part quality and productivity through the use of a high scan speed paired with a low hatch distance [153]. Similarly, Vaudreuil et al. analyzed the impact of laser power and scanning speed on the microstructure and mechanical properties of AlSi7Mg0.6, demonstrating that selecting mid-range laser power and scan speed within the optimal processing window enables the production of components with a refined microstructure and minimal defects [154]. The same outcomes were found by Mercurio et al., who investigated strategies to increase the production rate of PBF-LB/M for AlSi10Mg by optimizing critical process parameters. They found that the optimal combination of v and hd significantly reduced production time while preserving the material quality and performance [88]. In addition, they identified layer thickness as a key factor for improving process efficiency, especially for producing large-scale metal components [155]. In fact, in addition to the build time as defined by Tang. et al. [150], it is important to consider machine times such as lowering the platform, passing the recoater to spread a layer, raising the platform, processing the CAD for the upcoming slice, and starting lasing. Increasing the layer thickness reduces the number of slices to be lasered, which decreases recoater passes and machine times. However, despite the productivity gains, this method can lead to defects such as a lack of fusion between layers, which can result in stress concentration points that may be problematic under mechanical loading [149].

Another branch of the current literature focuses on advancing multi-laser systems capable of simultaneously melting multiple regions within the powder bed, thereby optimizing build rates and overall system efficiency [152]. Multi-laser systems employ multiple laser beams concurrently to melt materials, resulting in a substantial increase in productivity. High-power configurations offer significant efficiency improvements, particularly those utilizing dual or quad lasers. These systems provide key advantages, including the ability to process a wide range of materials and manufacture large components more cost-effectively [156]. Kasprowicz et al. demonstrated that using a machine with two lasers (whether both lasers are applied to a single sample or each laser works on separate models) can reduce build time by up to 50% compared to single-laser systems [149].

Commercial PBF-LB/M machines typically use a cartesian coordinate system with linear actuators positioned along three orthogonal axes. In this setup, parts are built vertically along one axis, the recoater moves along another axis, and the gas flow is managed along a third axis, sometimes parallel to the recoater movement. A notable drawback of this design is its need for sequential operation: the laser must pause during the movement of the axes, and the axes must pause during lasing [147]. To overcome this limitation, General Electric Company researchers have developed an innovative PBF-LB/M machine that uses a rotating powder bed and multiple scanning lasers, operating on a polar

coordinate system instead of the traditional cartesian system. This polar arrangement is particularly well-suited for manufacturing ring-like parts with large diameters and small cross-sections, which are common in the aerospace industry. In this sector, AM plays a crucial role in enhancing performance and reducing costs through innovative design and part consolidation [157]. Figure 10a–d illustrate the configurations of multi-laser cartesian and polar coordinate systems, as well as the components and outputs of the rotary powder bed fusion machine.

In rotary powder bed fusion machines, also referred to as spiral growth manufacturing [158], the system synchronizes the rotational movement of the powder bed with an ascending laser scanner and recoater to construct parts helically. A single-point powder feeder deposits metal powder near the inner radius of an annular build volume, while a recoater spreads the powder to the outer radius in a "snowplow" manner. Since the recoater and laser scanner operate at different angular locations, they function independently and simultaneously. This method has demonstrated build rates three times faster than traditional PBF-LB/M systems while reducing powder consumption by over fourfold [147,157,159]. Research by Ramos-Grez et al. on producing rings using 3D laser printing methods shows that the dimensional accuracy and the specific and nominal density of rings produced via polar printing are nearly identical to those achieved through cartesian methods. Additionally, the build rate efficiency of rings made with polar printing is approximately 5% higher than that of rings produced using the cartesian method [160].

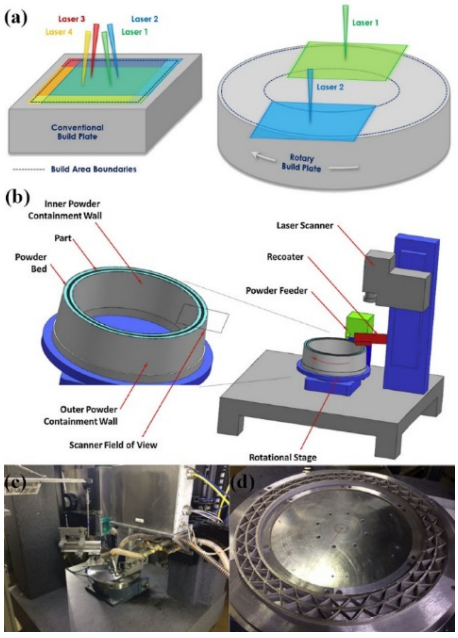

Figure 10. (**a**) Configuration of multi-laser cartesian and polar coordinate systems [159]: (**b**) rotational system components [157], (**c**) rotary PBF-LB/M system [147], and (**d**) example build [159].

Additional strategies to enhance PBF-LB/M productivity have been explored by Du Plessis et al., who investigated the use of shelled geometries combined with hot isostatic pressing (HIP) [161]. This approach focused on limiting laser melting to the outer shell or contour of the structure intentionally, leaving the interior powder unmelted. By reducing the volume of material that needs to be melted, this method significantly reduces PBF-LB/M production times. A subsequent HIP cycle, often required for ensuring structural reliability, then consolidates and densifies the entire part without adding extra costs, thereby improving both production speed and energy efficiency. Furthermore, Yim et al. identified that the shape of powder particles plays a key role in accelerating the PBF-LB/M process [162]. Specifically, they found that spherical particles enhance powder flowability,

promoting a more uniform distribution within the powder bed. In addition, the PSD was also observed to have a significant impact on productivity. In fact, a larger PSD generally results in faster printing due to improved flowability, further contributing to enhanced production efficiency.

4.2.3. Process Monitoring and Quality Control to Improve Component Life Service

In PBF-LB/M, the effective integration of process monitoring and quality control is pivotal for optimizing component longevity and advancing sustainability. Continuous monitoring of process parameters enables real-time detection of deviations that could result in defects like porosity or incomplete fusion. By employing rigorous quality control measures informed by this monitoring data, only components that adhere to stringent quality standards are produced, thereby reducing the risk of premature failure and extending service life. Additionally, minimizing defects and rework enhances component reliability and decreases material waste and energy consumption, thus contributing significantly to the sustainability of the PBF-LB/M process.

As mentioned in the previous section, enhancing the BR involves increasing the laser movement speed, which reduces energy density. Consequently, this raises the likelihood of producing parts with specific porosity defects, such as a lack of fusion [163]. Therefore, it is essential to ensure that higher productivity does not compromise the quality of the parts. These defects can reduce the lifespan of the parts, potentially leading to premature failure and disrupting the sustainability chain.

PBF-LB/M, like all conventional manufacturing methods, requires robust quality assurance procedures and advanced tools to effectively manage and certify the quality of fabricated components. In PBF-LB/M, the reliability and longevity of produced components are significantly influenced by factors such as defects, residual stresses, and microstructural inconsistencies [164]. Specifically, the PBF-LB/M process involves complex interactions between laser, powder, and substrate, and even minor deviations can lead to defects such as porosity, warping, or structural weaknesses [165]. Aluminum alloys processed by PBF-LB/M are characterized by a limited absorption of laser energy to the wavelength of YAG Laser, leading to inconsistent melting and promoting the formation of oxides, which can cause porosity and affect the mechanical properties of the final part [166]. Additionally, the rapid cooling rates associated with PBF-LB/M can induce significant residual stresses, resulting in distortion and cracking [167]. Effective monitoring and quality control are, therefore, imperative to address these challenges and enhance the service life and structural integrity of Al PBFed components. Both in situ (or in-line) monitoring techniques, which provide real-time data on process characteristics, and ex-line monitoring techniques, such as post-build inspection and analysis, play crucial roles in ensuring the quality and durability of these components.

In situ monitoring provides continuous oversight of process parameters and material behavior, enabling early detection of issues and facilitating immediate corrective actions. This real-time feedback loop is crucial for maintaining the desired quality and performance of the final parts. These techniques facilitate increased process efficiency by optimizing operational parameters such as laser power and scan speed using live data, thereby minimizing material waste and reducing production times. In addition, in situ monitoring reduces the necessity for extensive post-build inspections and rework by addressing potential issues during the build process. Moreover, it supports improved predictive maintenance by providing critical data on equipment wear and performance, which enhances equipment reliability and decreases downtime [164]. In PBF-LB/M, various in situ monitoring techniques are employed to ensure process quality, including optical, thermal, radiographic, and acoustic methods [164]: optical monitoring utilizes high-speed imaging and laser

scanning to observe melt pool dynamics and surface topology, which are crucial for layer uniformity and accuracy; thermal monitoring employs infrared cameras, thermocouples, and pyrometers to track temperature distributions and detect potential overheating or melting issues; radiographic techniques, including X-ray imaging and computed tomography, offer insights into internal structures and potential defects by visualizing the internal features of the melt pool and the solidified material; and acoustic monitoring involves ultrasonic sensors and microphones to analyze sound waves, helping to identify irregularities in melt pool behavior and powder deposition. Figure 11 illustrates the classification of defects in AM, along with monitoring techniques categorized into ex situ and in situ methods.

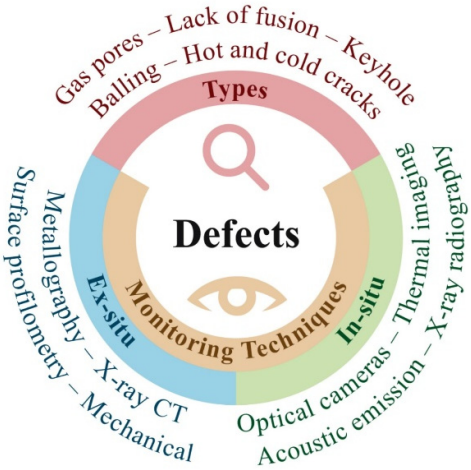

Figure 11. Overview of defect types in additive manufacturing and their monitoring techniques, categorized into ex situ and in situ methods.

Observing and analyzing melt pool characteristics in PBF-LB/M is critical for ensuring high-quality parts, as it facilitates real-time defect detection, process optimization, and control over microstructural properties. In addition, such monitoring also contributes to improvements in surface finish and dimensional accuracy [168]. Through the application of in situ monitoring and adaptive control strategies, manufacturers can achieve parts with enhanced mechanical properties, fewer defects, and greater reliability. The following delineates the specific benefits of real-time melt pool monitoring within the PBF-LB/M process. Defects commonly associated with PBF-LB/M, including porosity, a lack of fusion, and keyholing, are closely linked to deviations in melt pool behavior. For instance, porosity may arise when the melt pool is insufficiently deep or fails to fuse the powder layers completely. By scrutinizing the depth and stability of the melt pool, it is possible to adjust laser parameters to mitigate incomplete melting. Similarly, keyholing, which occurs due to excessive energy input, can result in deep and unstable melt pools, leading to significant defects. Effective observation of melt pool characteristics facilitates the early detection and rectification of these conditions, thereby improving the overall quality of the manufactured components. In Rees et al. [169], in situ X-ray imaging was employed to provide real-time visualization of the processes occurring during the PBF-LB/M of an Al-2139 alloy with TiB_2 additions. This advanced imaging technique enabled the observation of the rapid formation and evolution of hot cracks and porosity at the microscale, capturing critical details of crack propagation, laser-powder interactions, and pore dynamics within milliseconds. These real-time insights were pivotal in understanding the influence of various process parameters and material modifications on defect formation.

Not only does monitoring the melt pool aid in the early detection of defects but it also helps identify issues related to residual stress-induced defects. Residual stresses, which can cause warping or cracking of the manufactured part, are influenced by the thermal

gradients and cooling rates of the melt pool. By analyzing the melt pool temperature distribution and cooling rates, it is possible to optimize laser power, scanning speed, and path strategies to minimize thermal gradients and, consequently, residual stresses. The integration of an active contours image segmentation technique with a statistical process monitoring framework facilitates the automated detection of both in-plane and out-of-plane deviations from the nominal geometry on a layer-by-layer basis in real-time [170]. This monitoring approach is crucial for managing residual stresses and maintaining dimensional accuracy, as it enables the early identification of anomalies, such as local contaminations or distortions resulting from thermal stresses or material inconsistencies.

Beyond detecting defects and managing residual stresses, in situ melt pool monitoring is essential for gaining insights into the material properties of the final part. Numerous studies have shown that the microstructure, including grain size and phase composition, is largely determined by the solidification rate and thermal history of the melt pool [171,172]. By observing melt pool characteristics, process parameters can be adjusted to optimize cooling rates, which in turn directly influence the microstructure and mechanical properties of the part. For instance, faster cooling rates can result in finer microstructures leading to improved strength and hardness. Schmeiser et al. [173], through the use of synchrotron radiation, investigated the effects of different laser powers and scanning speeds affected crystallographic texture and lattice defects. Their findings revealed that higher laser power and scan speed promoted a strong crystallographic orientation, while lower settings did not.

Although the importance of real-time monitoring of melt pool characteristics is long-established, the importance of maintaining a feedback loop cannot be underestimated. Real-time feedback allows for adaptive process control, where laser parameters (such as power, speed, and focus) are dynamically adjusted based on the observed melt pool behavior. This dynamic adjustment ensures that melt pool conditions remain consistent, which is crucial for achieving uniform part quality and minimizing defects. A study explored the implementation of a feedback control system in layer-wise laser melting processes, utilizing optical sensors to enhance process precision [174]. The research specifically focused on monitoring the melt pool thermal profile through infrared thermography. This technique enables the real-time observation of thermal deviations from the target temperature profile. When such deviations are detected, the system dynamically adjusts the laser power to correct the temperature discrepancies. This feedback mechanism is crucial for maintaining a stable thermal environment within the melt pool, thereby promoting uniform part quality and mitigating common defects, such as porosity and cracking.

The quality of the melt pool also affects the surface finish and dimensional accuracy of the printed parts. It was proved that a stable and well-controlled melt pool results in smoother surfaces and better adherence to the intended geometry. In a study [168], advanced in situ monitoring systems, including coaxial high-speed cameras and off-axis imaging, were employed to observe and record the behavior of the melt pool during the PBF-LB/M process. These systems captured essential data such as melt pool temperature and intensity. The gathered data were utilized to construct detailed melt pool signature maps, which were subsequently integrated into a neural network model to predict the surface topography of the printed layers accurately. By identifying melt pool temperature as a critical predictor of surface characteristics, the study facilitated real-time adjustments to process parameters, such as laser power and scanning speed. A comprehensive review of the published studies related to in situ monitoring techniques utilized in metal powder bed fusion was carried out by Grasso et al. [175]. The authors detailed how the continuous analysis of melt pool characteristics enhances the understanding of the interplay between process parameters and material properties. This insight is crucial for the refinement of process parameters, thereby contributing to improved repeatability and reliability in the

production of high-quality components. In addition, data collected from real-time melt pool monitoring can be used to develop predictive models and simulations that can guide the initial parameter settings and reduce the need for trial-and-error approaches, thus streamlining the development process and reducing time and material waste.

5. Post-Processing

5.1. Redesign Heat Treatment for a Sustainable PBF-LB/M Manufacturing

The rapid advancements in PBF-LB/M technology have driven significant interest in optimizing post-processing methods, particularly heat treatments, to enhance the performance of aluminum components. Unlike conventional methods, the PBF-LB/M process induces unique metallurgical characteristics due to its extremely high cooling rates (in the range of 10^3–10^7 K/s), and successive heating and cooling cycles due to the layer-by-layer construction. These features lead to the formation of strongly supersaturated solid solutions (SSSSs), generation of residual stresses, and epitaxial growth on the underlying layers, which results in directional solidification and mechanical anisotropy and in situ heat treatment of previously solidified material, which in turn causes local phase transformations and precipitation [176]. Given these distinctive characteristics, conventional heat treatments, which are typically optimized for slowly solidified alloys, may not be directly applicable. Their long durations and high temperatures, though effective for conventional alloys, are likely not suitable for PBFed components, as they do not account for the microstructural peculiarities induced by rapid solidification. Moreover, the environmental impact of traditional heat treatments, which require significant energy and extended processing times, adds an additional layer of concern. Therefore, there exists a pressing need to develop novel heat treatments specifically tailored to PBFed aluminum alloys that must be shorter and more energy-efficient to reduce the environmental footprint while simultaneously being capable of achieving the desired microstructural and mechanical properties.

As mentioned above, the PBF-LB/M process enables a favorable SSSS condition in the as-built state, thanks to the high cooling rates characteristic of this technology. This feature allows an increased amount of solute in solution, even for elements with low solubility in aluminum, sometimes exceeding the levels achievable through conventional solution treatment and quenching. For example, it has been demonstrated that Al-Si-Mg alloys processed via PBF-LB/M exhibit higher supersaturation compared to that obtained with traditional thermal treatments [177]. In addition, Babu et al. exploited this PBF-LB/M peculiarity to produce a high solute Al–Zn–Mg alloy with 14 wt% Zn and 3 wt% Mg where excess manganese was added to improve the solid solution strengthening of the alloy, in addition to second-phase strengthening produced by Sc [178]. Furthermore, Jia et al. observed that the exceptionally high cooling rates achievable in the PBF-LB/M process can retain up to 4.3 wt% of Mn in supersaturated solid solution within Al-Mn alloys—significantly surpassing its equilibrium solubility of approximately 1.8 wt% [179]. This phenomenon was leveraged by Martucci et al. to develop a novel Al-Mn-Cr-Zr alloy containing 5 wt% Mn, which exhibited exceptional solid solution strengthening and achieved high hardness in the as-built condition [180]. The increased SSSS characteristic of the PBF-LB/M process opens up the possibility of using aluminum-based alloys in the as-built state or with reduced treatments, leveraging supersaturation to achieve fast and effective strengthening through artificial aging. In this context, mechanical strengthening occurs via the precipitation of coherent and semi-coherent nanometric particles, making some Al-based alloys particularly suitable for direct use after faster heat treatment without requiring preliminary long solution treatment. Reducing heat treatments required on PBFed Al-based alloys further lessens energy consumption and reduces greenhouse gas emissions due to energy being produced by fossil fuels. Such direct processes preserve the

material properties, reduce the occurrence of defects, and limit reprocessing requirements; hence, the whole circle of manufacturing time is reduced and greener. Higher throughputs and better use of resources further optimize production efficiency. This aligns well with the industrial goal of sustaining manufacturing with a low environmental impact.

One traditional post-processing treatment in the AM sector that delivers superior mechanical properties while minimizing processing time and reducing overall costs is direct aging, also known as T5 temper [181,182]. This approach is particularly effective for alloys like Al-Cu, Al-Zn-Mg, and Al-Mg-Sc, which exhibit significant hardening potential when subjected to aging treatments [176]. Unlike solution treatment followed by aging, direct aging capitalizes on the supersaturation of alloying elements achieved through rapid solidification, enabling enhanced precipitation hardening. For instance, in Al-Mg-Sc alloys, direct aging has demonstrated a 72 HV increase in hardness due to additional Al_3Sc precipitate formation [183]. T5 on Al-Mg-Sc alloys effectively improves yield strength, elevating it from 362 MPa in the as-built condition to 520 MPa after aging at 350 °C for 2 h [184]. Conversely, in Al-Si-Mg alloys, the effects of direct aging are more subdued, with only slight improvements in mechanical behavior and limited impact on residual stress or grain size. While T5-treated Al-Si-Mg samples exhibit the highest mechanical resistance among various heat treatments, the deviation from as-built properties is less pronounced compared to that achieved in solution-treated samples [185]. However, direct aging in Al-Si alloys can reduce toughness by 35–40%, altering the fracture behavior to be more random and less localized at melt pool boundaries [186]. The T5 treatment can also be performed in situ by leveraging platform pre-heating during the PBF-LB/M process, offering a streamlined and sustainable approach to enhance material properties directly during fabrication. For instance, Raffeis et al. [187] investigated the precipitation of various Al-Cu-Li phases in a PBFed 2099 alloy. The study compared the effects of in situ treatment, achieved by pre-heating the build platform to 220, 320, and 520 °C. In situ treatments successfully induced the precipitation of hardening phases. Bosio et al. [188] investigate the feasibility of conducting in situ heat treatments during the PBF-LB/M process for AlSi10Mg components. Conventional PBF-LB/M systems typically operate with build plate temperature limits of 200 to 250 °C, restricting their application to in situ aging and low-temperature stress relief. In their work, the authors elevated the build plate temperature to 500 °C during 10–13 h of printing. At 220 °C, extended build times facilitated an in situ direct aging heat treatment, while printing at 300 °C enabled effective stress relief. Furthermore, temperatures of 450 and 500 °C allowed the implementation of in situ solution heat treatments. Schimback et al. [189] examine the in situ heat treatment of Scalmalloy® within the PBF-LB/M process. The build platform was heated to 200 °C, promoting the formation of Sc solute clusters. The presence of strength-enhancing secondary particles in the specimens produced under these conditions resulted in mechanical properties comparable to those of peak-aged Scalmalloy®. The in situ heat treatments are not only efficient but also more sustainable, as they reduce the energy and time associated with separate post-processing steps. By integrating heat treatment into the printing process, energy-intensive post-build furnaces can be avoided, and the overall carbon footprint of the manufacturing process is significantly lowered, aligning with broader goals of environmental sustainability in advanced manufacturing.

In addition to enhancing material properties, platform pre-heating can also help alleviate residual stresses, which are a common challenge in PBF-LB/M processes due to the rapid thermal cycling that occurs during printing. The high temperatures and rapid cooling cycles inherent in these processes induce residual stresses that can lead to distortion, warping, or cracking if not properly managed. Pre-heating the platform helps mitigate these stresses by providing a more controlled thermal gradient, reducing the cooling rates that contribute to stress accumulation. However, while pre-heating can offer some relief,

it is often still necessary to apply a dedicated post-processing heat treatment at elevated temperatures to fully alleviate residual stresses. Such heat treatments must be carefully designed to balance stress reduction with the preservation of the material microstructure and mechanical properties. For example, in Al-Si-Mg alloys, stress-relieving temperatures are often a challenge because precipitation hardening typically occurs at temperatures between 150–200 °C, which is insufficient to effectively relieve residual stresses after PBF-LB/M. While a typical stress-relieving treatment of 2 h at 300 °C helps soften the alloy, it also reduces strength, necessitating a subsequent solution heat treatment to regain mechanical properties [190].

While it is true that the current literature is progressively shifting toward shorter, simpler, and more sustainable heat treatments to align with environmental and economic demands, more comprehensive treatments, such as the T6 process, which includes solution heat treatment followed by aging, remain essential in some instances. Specifically, the T6 treatment is often necessary to mitigate the effects of microstructural anisotropy introduced by the PBF-LB/M process. This anisotropy, inherent to layer-by-layer manufacturing, can lead to heterogeneities in mechanical performance, such as reduced toughness or non-uniform elongation. Moreover, T6 treatments are particularly beneficial for enhancing the toughness and elongation at fracture of additively manufactured components, properties that are frequently challenging to optimize in metal AM. Despite the increasing emphasis on leaner thermal treatments, the trade-off in mechanical performance must be carefully evaluated to ensure the reliability and functionality of components in demanding applications. However, the as-printed SSSS condition of additively manufactured components can significantly reduce the duration required for the solutionizing step in the T6 treatment. This feature allows for shorter heat treatment cycles, reducing energy consumption and enhancing the overall sustainability of the process, without compromising the benefits of the T6 approach. For example, Vanzetti et al. investigated the effects of a shortened T6 heat treatment on PBF-LB/M AlSi7Mg samples [191]. The procedure involved a 15 min solution treatment at 540 °C, followed by water quenching and artificial aging at 170 °C for 2–8 h. The results demonstrate that the shorter solution treatment effectively dissolves the fine phases generated during the PBF-LB/M process. However, the subsequent aging at 170 °C for 6 h leads to tensile properties that are slightly lower than those obtained with the standard T6 treatment. Di Egidio et al. examined a novel rapid T6 heat treatment for AlSi10Mg alloy produced via PBF-LB/M, comparing its performance with T5 and conventional T6 heat treatments [192]. This rapid T6 process includes a brief solution treatment (10 min at 510 °C) followed by artificial aging (6 h at 160 °C). The objective of this treatment is to homogenize the microstructure and relieve residual stresses in the as-built alloy while preserving its fine microstructural features and associated strengthening mechanisms. The shortened solution treatment reduces porosity growth typically seen at elevated temperatures, resulting in a uniform dispersion of fine globular Si particles within the aluminum matrix. Moreover, this approach limits diffusion, increasing the amount of Mg and Si in solid solution, thereby enhancing precipitation hardening while preventing microstructural coarsening. ASTM F3318-18 specifies the properties of finished PBF-LB/M AlSi10Mg parts and includes guidelines for thermal processing techniques such as stress relieving, solution heat treatment, T6 tempering, and HIP [64]. HIP applies high temperatures, typically above 70% of the material melting point, combined with isostatic pressure, up to approximately 200 MPa, in a gas medium such as argon or nitrogen. HIP is primarily used to close internal pores and correct internal defects, thereby enhancing overall material performance, though it has limited effectiveness on surface-connected defects, such as surface pores [193].

Recent advancements in AM have led to the development of novel aluminum alloys specifically optimized for PBF-LB/M processes, which eliminate the need for post-

processing heat treatments like T5, T6, or HIP. These new alloys are engineered to deliver high strength, toughness, and ductility directly from the build process, reducing production time and costs while streamlining the manufacturing workflow. This breakthrough not only enhances efficiency and sustainability but also mitigates the risks of part distortion and microstructural degradation associated with traditional thermal processing. As a result, industries such as aerospace, automotive, and tooling benefit from faster production cycles, reduced energy consumption, and improved part quality, marking a significant advancement in AM technology. As mentioned in Section 4.1.1, Elementum 3D has developed enhanced versions of traditional alloys using its RAM technology, which incorporates ceramic nanoparticles to improve printability. The company launched aluminum alloys A5083-RAM2™ and A5083-RAM5™, featuring 2 and 5% volume of RAM additives, respectively, to the A5083 alloy. These high-strength aluminum alloys offer excellent printability and good corrosion resistance and do not require post-build heat treatment. For instance, A5083-RAM5 consistently exhibits uniform tensile properties in both horizontal and vertical orientations, whether in the as-printed or stress-relieved states. The inclusion of RAM additives substantially increases its strength relative to conventional wrought 5083 alloys. Specifically, in the as-printed condition, A5083-RAM5 achieves 1.8 times the yield strength of strain-hardened wrought 5083-H116, and in the stress-relieved state, it attains 2.9 times the yield strength of wrought 5083-O [194]. Figure 12 compares various heat treatment methods for PBFed aluminum alloys, highlighting their effectiveness in enhancing material properties and energy efficiency.

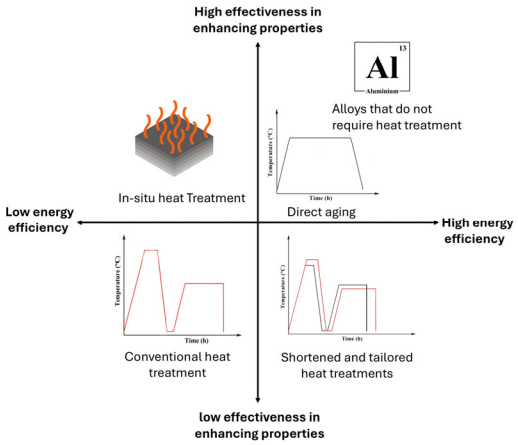

Figure 12. Comparison of energy efficiency and property enhancement across various heat treatment methods for PBFed aluminum alloys.

5.2. Strategies to Reduce Surface Post-Processing Operations

Managing surface roughness during manufacturing is essential for producing ready-to-use components, minimizing the need for extensive post-processing. When compared to subtractive manufacturing, the limited surface finish and dimensional accuracy of PBFed aluminum components restrict their broader adoption. For this reason, optimizing PBF-LB/M process parameters is crucial for enhancing surface quality, which directly affects the mechanical performance and dimensional accuracy of 3D-printed parts [195]. By fine-tuning the PBF-LB/M parameters, smoother surfaces can be achieved, significantly reducing the reliance on post-processing methods like machining or polishing [196]. This approach not only boosts production efficiency but also promotes sustainability by conserving energy, minimizing material waste, and lowering the overall carbon footprint. Surface roughness refers to the micro-scale irregularities on a material surface and is a critical factor for the mechanical properties, especially for dynamic ones such as fatigue strength [197,198]. The literature has amply demonstrated that surface roughness is pre-

dominantly influenced by three key factors: irregular solidification of the melt pool driven by process dynamics, the adhesion of powder particles to the surface, and the staircase effect [199–201]. There are various methods for characterizing and quantifying surface roughness, with the most widely used relying on mathematical parameters that describe the surface profile. Roughness values can be calculated either along a single profile (line) or across an entire surface (area). These parameters are generally classified into three categories based on their function: amplitude parameters, spacing parameters, and hybrid parameters. The most used surface roughness parameter for PBF-LB/M components is Ra, also referred to as the arithmetic average height or center line average. Ra is widely accepted in general quality control, representing the average absolute deviation of surface irregularities from the mean line over a defined sampling length [201].

Attaining the desired surface quality and dimensional precision necessitates the careful selection of appropriate PBF-LB/M parameter combinations. Li et al. demonstrated that the variation in surface quality of 7075 alloy samples is significantly influenced by both laser power and volume energy density [202]. In particular, they observed that by keeping constant the scan speed, surface roughness consistently decreased with increasing laser power. A parabolic trend was instead seen by correlating surface roughness with Volumetric Energy Density (VED), a crucial parameter that combines several process parameters (laser power, scanning speed, hatch spacing, and layer thickness) to provide an integrated measure of energy applied per unit volume of the powder bed. The roughest surface was observed at a low energy density of VED = 43 J/mm^3, while a smooth, dense surface was obtained at VED = 313 J/mm^3, and a relatively rough surface at a high energy density of VED = 1565 J/mm^3. The same trend was noticed by Li et al. [203] on AlSi10Mg parts. They investigated the correlation between VED and surface roughness, paying attention to the effects on the five faces of the PBFed cubes. Their study demonstrated that as energy density increased, the roughness of the five faces initially decreased before rising again, whereas the roughness of the top surface exhibited a slight increase. The most favorable surface quality was achieved at energy densities of 175 and 200 J/mm^3. In another study on the surface roughness of PBFed AlSi7Mg, the findings showed that laser power and scan speed significantly impacted surface roughness [204]. Another parameter that influences surface roughness is the use of contour scans. The material is melted along paths parallel to the component contour, either before or after the infill. The scan parameters can be optimized to reduce surface roughness. In general, it was stated that higher energy input ensures more uniform melt tracks, smoothing out peaks and valleys through re-melting [199]. Musekamp et al. [205] investigated the impact of contour parameters on surface roughness and their effect on the fatigue performance of PBFed Scalmalloy®. They stated that the application of optimized contour parameters yielded a 10–20% improvement in fatigue properties compared to the condition without contour scans. Most research has focused on the roughness of the top face of components, while some studies have also examined the roughness of other faces and overhanging surfaces. Yang et al. [206] conducted a study to assess the impact of process parameters on the overhanging surface roughness of AlSi10Mg specimens fabricated without support structures, at various build angles (30, 45, and 60°). The parameters analyzed included infill laser power, infill scanning speed, infill scanning angle, contour laser power, and contour scanning speed. The findings revealed that contour process parameters exerted a significantly greater influence on surface roughness compared to infill parameters. Moreover, the effect of these parameters on surface roughness decreased as the build angle increased, with contour scanning speed identified as the most critical factor. In order to reduce as much as possible experimental studies with consequent waste of dust, energy, and cost, a lot of attention is currently being paid to the development of models based on machine learning techniques to predict how

various parameter combinations impact surface roughness and dimensional accuracy in the final PBFed components [207].

Although process parameter optimization has proven to be a successful ally in optimizing the component surface roughness by maximizing its dynamic mechanical properties and limiting post-processing operations, the average roughness in PBF-LB/M production is always above the 3.2 μm required in aerospace applications [208]. In addition, post-processing machining becomes necessary when contact surfaces are present or when the dynamic properties of the component are particularly stressed during service [209]. Such a need is rendered particularly pronounced when Al-based alloys are involved. In fact, Al-based alloys processed for PBF-LB/M have been shown to have much higher surface roughness than Ni-, Ti-, or steel-based alloys, making them inapplicable in specific industrial applications [131]. In order to undergo post-processing operations, the component must be detached from the additive platform, brought onto a workbench, and subjected to one or more machining operations with possible repositioning. This results in laborious manual operations, downtime, and additional costs, making the process unsustainable.

Hybrid manufacturing, which encompasses various combinations of processes and mechanisms, plays a pivotal role in enhancing sustainability by optimizing material usage, reducing energy consumption, and streamlining production stages. This approach effectively addresses the productivity challenges associated with traditional AM, such as extended production times and high per-unit costs, by leveraging the strengths of multiple manufacturing techniques. By consolidating production steps and minimizing the number of machines required, hybrid manufacturing not only improves operational efficiency but also strongly aligns with sustainability goals, promoting resource conservation and waste reduction [210,211]. In hybrid AM, additive processes are combined with subtractive techniques, such as CNC machining, to optimize material properties, precision, and dimensional tolerances [212]. While current hybrid additive–subtractive technologies have primarily focused on combining direct energy deposition with machining processes, the integration of PBF-LB/M with CNC milling presents a promising solution to overcoming the challenges of surface finish and precision [213]. Several companies have developed hybrid manufacturing systems that combine PBF-LB/M methods with CNC milling, enabling the production of faster and more complex parts. Matsuura has pioneered this technology with its LUMEX Avance-25, an innovative hybrid CNC machine that integrates 3D printing, metal laser sintering, and milling. This cutting-edge system enables the production of intricate metal components with superior surface finishes [214]. Since entering the market in 2017, Sodick has emerged as a leader in hybrid manufacturing. Their OPM250L and OPM350L models seamlessly integrate selective laser melting and high-speed milling, facilitating the production of complex metal molds with exceptional precision and finish. This advanced technology significantly boosts productivity, reduces lead times, and lowers costs compared to conventional manufacturing methods [215]. Liu et al. developed a hybrid system integrating PBF-LB/M with a three-axis CNC milling machine [209]. PBF-LB/M with CNC milling systems are primarily employed in the mold industry, taking advantage of their ability to consolidate most, if not all, manufacturing processes within a single machine. They are particularly suited for the production of medium to large parts, such as conformal cooling channels in molds, which optimize cooling efficiency and are nearly impossible to produce as single components using conventional methods. Furthermore, these systems help reduce the likelihood of defects caused by limited access to cutting tools. In mold manufacturing, it is crucial for the cooling medium to flow with minimal resistance, necessitating exceptionally smooth surfaces in the cooling channels. This level of surface finish can only be achieved through CNC machining, rather than AM [216].

6. Summary and Perspectives

Global industrial production significantly contributes to greenhouse gas emissions, with aluminum manufacturing standing out for its high energy intensity. This issue is compounded by rising demand due to economic growth and population increases. Tackling the environmental impact of aluminum traditional production is critical, as global warming, largely driven by CO_2 emissions from industries, manufacturing, and transportation, remains one of the world most urgent challenges. PBF-LB/M additive technology has emerged as a transformative solution for advancing sustainability by optimizing material use, incorporating industrial waste, and reducing energy consumption and emissions. Despite its benefits, AM energy-intensive nature highlights the need for further advancements in energy efficiency to achieve its full sustainability potential.

This review examined how PBF-LB/M can address environmental challenges by enhancing material efficiency, minimizing waste, and optimizing energy use in aluminum-based alloy production. Aluminum lightweight and recyclable properties, combined with the design flexibility and efficiency of PBF-LB/M, establish it as a key driver of sustainable innovation. The paper explores strategies to improve PBF-LB/M sustainability across the entire process chain, from feedstock production to post-processing.

- The production of metal powders for PBF-LB/M is energy-intensive, with environmental impacts varying by fabrication methods and feedstock sources. Conventional techniques like gas and water atomization or plasma-based processes balance energy use, particle morphology, and costs. Emerging methods, such as cold mechanically derived powders and UniMelt® plasma technology, offer more sustainable alternatives by enabling high-yield, low-energy production and efficient recycling of feedstocks. Incorporating recycled materials into powder production further decreases CO_2 emissions and conserves natural resources. Additionally, the reuse of PBF-LB/M powders across multiple build cycles, supported by rigorous quality control measures, including blending, sieving, and property monitoring, enhances sustainability and economic viability.
- PBF-LB/M revolutionizes sustainable manufacturing by integrating lightweight materials with advanced designs. Innovations in tailored alloy compositions and modifications to traditional alloys address challenges like hot cracking, enabling the production of components with superior strength, ductility, and thermal stability. Structural design techniques, such as topology optimization and lattice structures, enhance material efficiency, reduce weight, and improve performance, key benefits for aerospace and automotive applications. Process optimization methods, including DoE and single scan track analysis, reduce defects, energy consumption, and material waste while ensuring dense, durable parts. Additionally, advancements like parameter optimization, multi-laser systems, polar coordinate designs, and real-time melt pool monitoring enhance productivity, quality, and component lifespan.
- Integrating tailored post-processing techniques with the PBF-LB/M process is critical for achieving sustainability and improving material performance. Traditional heat treatments, often energy-intensive, are being replaced by accelerated heat treatments that reduce processing time and energy consumption without compromising material properties. Recent advancements propose shorter, more energy-efficient treatments that optimize mechanical properties while minimizing environmental impact and production costs. Additionally, reducing surface post-processing through parameter optimization and hybrid manufacturing approaches further enhances efficiency and sustainability.

In conclusion, PBF-LB/M holds substantial potential to drive sustainability advancements across industrial and mobility sectors. By optimizing design processes to reduce

material consumption, implementing material recycling, managing energy use, minimizing post-processing requirements, conducting comprehensive life cycle assessments, and fostering cross-industry collaboration, manufacturers can substantially lower their environmental footprint. While challenges such as energy intensity, the limited scalability of PBF-LB/M, and the environmental impact of raw material preparation remain, the potential of additive processing of aluminum alloys to revolutionize sustainable manufacturing is immense. Continued innovation in process optimization, material development, and integration of renewable energy sources will be crucial.

Author Contributions: Conceptualization, A.M., S.B., D.U., L.M., P.F. and M.L.; resources, M.J.Y.; writing—original draft preparation, M.J.Y. and A.M.; writing—review and editing, M.J.Y., A.M. and M.L.; visualization, S.B., D.U., L.M., P.F. and M.L.; supervision, S.B., D.U., L.M., P.F. and M.L.; project administration, M.L.; funding acquisition, M.L. All authors have read and agreed to the published version of the manuscript.

Funding: Financed by the European Union—NextGenerationEU (National Sustainable Mobility Center CN00000023, Italian Ministry of University and Research Decree n. 1033-17/06/2022, Spoke 11—Innovative Materials & Lightweighting). The opinions expressed are those of the authors only and should not be considered representative of the European Union or the European Commission's official position. Neither the European Union nor the European Commission can be held responsible for them.

Institutional Review Board Statement: Not applicable.

Informed Consent Statement: Not applicable.

Data Availability Statement: No new data were created or analyzed in this study.

Conflicts of Interest: The authors declare no conflicts of interest.

References

1. Filonchyk, M.; Peterson, M.P.; Zhang, L.; Hurynovich, V.; He, Y. Greenhouse Gases Emissions and Global Climate Change: Examining the Influence of CO_2, CH_4, and N_2O. *Sci. Total Environ.* **2024**, *935*, 173359. [CrossRef] [PubMed]
2. United States Environmental Protection Agency Sources of Greenhouse Gas Emissions. Available online: https://www.epa.gov/ghgemissions/sources-greenhouse-gas-emissions (accessed on 1 December 2024).
3. Filonchyk, M.; Peterson, M.P.; Yan, H.; Gusev, A.; Zhang, L.; He, Y.; Yang, S. Greenhouse Gas Emissions and Reduction Strategies for the World's Largest Greenhouse Gas Emitters. *Sci. Total Environ.* **2024**, *944*, 173895. [CrossRef] [PubMed]
4. Nunes, L.J.R. The Rising Threat of Atmospheric CO_2: A Review on the Causes, Impacts, and Mitigation Strategies. *Environments* **2023**, *10*, 66. [CrossRef]
5. Elkington, J. Towards the Sustainable Corporation: Win-Win-Win Business Strategies for Sustainable Development. *Calif. Manag. Rev.* **1994**, *36*, 90–100. [CrossRef]
6. Wang, Y.; Peng, T.; Xiong, Y.; Kim, S.; Zhu, Y.; Tang, R. An Ontology of Eco-Design for Additive Manufacturing with Informative Sustainability Analysis. *Adv. Eng. Inform.* **2024**, *60*, 102430. [CrossRef]
7. Winter, S.; Quernheim, N.; Arnemann, L.; Anderl, R.; Schleich, B. Live Estimating the Carbon Footprint of Additively Manufactured Components—A Case Study. *Procedia CIRP* **2023**, *116*, 642–647. [CrossRef]
8. Fredriksson, C. Sustainability of Metal Powder Additive Manufacturing. In *Procedia Manufacturing*; Elsevier B.V.: Amsterdam, The Netherlands, 2019; Volume 33, pp. 139–144.
9. Ford, S.; Despeisse, M. Additive Manufacturing and Sustainability: An Exploratory Study of the Advantages and Challenges. *J. Clean. Prod.* **2016**, *137*, 1573–1587. [CrossRef]
10. Colorado, H.A.; Velásquez, E.I.G.; Monteiro, S.N. Sustainability of Additive Manufacturing: The Circular Economy of Materials and Environmental Perspectives. *J. Mater. Res. Technol.* **2020**, *9*, 8221–8234. [CrossRef]
11. Aboulkhair, N.T.; Simonelli, M.; Parry, L.; Ashcroft, I.; Tuck, C.; Hague, R. 3D Printing of Aluminium Alloys: Additive Manufacturing of Aluminium Alloys Using Selective Laser Melting. *Prog. Mater. Sci.* **2019**, *106*, 100578. [CrossRef]
12. Stojanovic, B.; Bukvic, M.; Epler, I. Application of Aluminum and Aluminum Alloys in Engineering. *Appl. Eng. Lett.* **2018**, *3*, 52–62. [CrossRef]

13. Al-Alimi, S.; Yusuf, N.K.; Ghaleb, A.M.; Lajis, M.A.; Shamsudin, S.; Zhou, W.; Altharan, Y.M.; Abdulwahab, H.S.; Saif, Y.; Didane, D.H.; et al. Recycling Aluminium for Sustainable Development: A Review of Different Processing Technologies in Green Manufacturing. *Results Eng.* **2024**, *23*, 102566. [CrossRef]
14. Li, S.; Yue, X.; Li, Q.; Peng, H.; Dong, B.; Liu, T.; Yang, H.; Fan, J.; Shu, S.; Qiu, F.; et al. Development and Applications of Aluminum Alloys for Aerospace Industry. *J. Mater. Res. Technol.* **2023**, *27*, 944–983. [CrossRef]
15. Mazzolani, F.M. Structural Applications of Aluminium in Civil Engineering. *Struct. Eng. Int.* **2006**, *16*, 280–285. [CrossRef]
16. Kumar Dalapati, G.; Masudy-Panah, S.; Kumar, A.; Cheh Tan, C.; Ru Tan, H.; Chi, D. Aluminium Alloyed Iron-Silicide/Silicon Solar Cells: A Simple Approach for Low Cost Environmental-Friendly Photovoltaic Technology. *Sci. Rep.* **2015**, *5*, 17810. [CrossRef] [PubMed]
17. Demirkesen, A.; Uçar, M. Investigation of the Effects of Using Aluminum Alloys in Electric Vehicles Production. 2020. Available online: https://www.researchgate.net/publication/348116085_Investigation_of_the_Effects_of_Using_Aluminum_Alloys_in_Electric_Vehicles_Production (accessed on 26 September 2024).
18. Wang, D.; Liu, L.; Deng, G.; Deng, C.; Bai, Y.; Yang, Y.; Wu, W.; Chen, J.; Liu, Y.; Wang, Y.; et al. Recent Progress on Additive Manufacturing of Multi-Material Structures with Laser Powder Bed Fusion. *Virtual Phys. Prototyp.* **2022**, *17*, 329–365. [CrossRef]
19. Noronha, J.; Leary, M.; Brandt, M.; Qian, M. AlSi10Mg Hollow-Strut Lattice Metamaterials by Laser Powder Bed Fusion. *Mater. Adv.* **2024**, *5*, 3751–3770. [CrossRef]
20. Kavousi Sisi, A.; Ozherelkov, D.; Chernyshikhin, S.; Pelevin, I.; Kharitonova, N.; Gromov, A. Functionally Graded Multi-Materials by Laser Powder Bed Fusion: A Review on Experimental Studies. *Prog. Addit. Manuf.* **2024**. [CrossRef]
21. Dopler, M.; Weiß, C. Energy Consumption in Metal Powder Production. *BHM Berg- Hüttenmännische Monatshefte* **2021**, *166*, 2–8. [CrossRef]
22. Kellens, K.; Baumers, M.; Gutowski, T.G.; Flanagan, W.; Lifset, R.; Duflou, J.R. Environmental Dimensions of Additive Manufacturing: Mapping Application Domains and Their Environmental Implications. *J. Ind. Ecol.* **2017**, *21*, S49–S68. [CrossRef]
23. IEA. *Direct CO_2 Emissions from Industry in the Net Zero Scenario*; IEA: Paris, France, 2023.
24. *ISO ISO/UNDP PAS 53002:2024*; Guidelines for Contributing to the United Nations Sustainable Development Goals (SDGs). ISO: Geneva, Switzerland, 2024.
25. Fankhauser, S.; Smith, S.M.; Allen, M.; Axelsson, K.; Hale, T.; Hepburn, C.; Kendall, J.M.; Khosla, R.; Lezaun, J.; Mitchell-Larson, E.; et al. The Meaning of Net Zero and How to Get It Right. *Nat. Clim. Change* **2022**, *12*, 15–21. [CrossRef]
26. IPCC. *Global Warming of 1.5 °C*; Cambridge University Press: Cambridge, UK, 2018.
27. IEA. *Energy System—Transport*; IEA: Paris, France, 2023.
28. CRU Consulting. *Opportunities for Aluminium in a Post-COVID Economy—Prepared for the International Aluminium Institute*; CRU International Ltd.: London, UK, 2022.
29. *ISO 14067:2018*; Greenhouse Gases—Carbon Footprint of Products—Requirements and Guidelines for Quantification. ISO: Geneva, Switzerland, 2018.
30. *ISO 14040:2006*; Environmental Management—Life Cycle Assessment—Principles and Framework. ISO: Geneva, Switzerland, 2006.
31. Gebler, M.; Schoot Uiterkamp, A.J.M.; Visser, C. A Global Sustainability Perspective on 3D Printing Technologies. *Energy Policy* **2014**, *74*, 158–167. [CrossRef]
32. Huang, R.; Riddle, M.; Graziano, D.; Warren, J.; Das, S.; Nimbalkar, S.; Cresko, J.; Masanet, E. Energy and Emissions Saving Potential of Additive Manufacturing: The Case of Lightweight Aircraft Components. *J. Clean. Prod.* **2016**, *135*, 1559–1570. [CrossRef]
33. Weiss, C.; Bödger, C.; Ekkehard, S.; Heußen, D.; Häfner, C. Evaluation of the Ecological Footprint for Parts from AlSi10Mg Manufactured by Laser Powder Bed Fusion. In Proceedings of the International Solid Freeform Fabrication Symposium (2022), Austin, TX, USA, 25–27 July 2022.
34. Ingarao, G.; Priarone, P.C.; Deng, Y.; Paraskevas, D. Environmental Modelling of Aluminium Based Components Manufacturing Routes: Additive Manufacturing versus Machining versus Forming. *J. Clean. Prod.* **2018**, *176*, 261–275. [CrossRef]
35. Priarone, P.C.; Lunetto, V.; Atzeni, E.; Salmi, A. Laser Powder Bed Fusion (L-PBF) Additive Manufacturing: On the Correlation between Design Choices and Process Sustainability. *Procedia CIRP* **2018**, *78*, 85–90. [CrossRef]
36. Kravchenko, M.; Pigosso, D.C.A.; McAloone, T.C. Circular Economy Enabled by Additive Manufacturing: Potential Opportunities and Key Sustainability Aspects. In *Balancing Innovation and Operation*; The Design Society: Glasgow, UK, 2020.
37. Peng, T.; Wang, Y.; Zhu, Y.; Yang, Y.; Yang, Y.; Tang, R. Life Cycle Assessment of Selective-Laser-Melting-Produced Hydraulic Valve Body with Integrated Design and Manufacturing Optimization: A Cradle-to-Gate Study. *Addit. Manuf.* **2020**, *36*, 101530. [CrossRef]
38. Salmi, A.; Vecchi, G.; Atzeni, E.; Iuliano, L. Hybrid Multi-Criteria Decision Making for Additive or Conventional Process Selection in the Preliminary Design Phase. *Designs* **2024**, *8*, 110. [CrossRef]
39. Yi, L.; Glatt, M.; Sridhar, P.; de Payrebrune, K.; Linke, B.S.; Ravani, B.; Aurich, J.C. An Eco-Design for Additive Manufacturing Framework Based on Energy Performance Assessment. *Addit. Manuf.* **2020**, *33*, 101120. [CrossRef]

40. Guarino, S.; Ponticelli, G.S.; Venettacci, S. Environmental Assessment of Selective Laser Melting Compared with Laser Cutting of 316L Stainless Steel: A Case Study for Flat Washers' Production. *CIRP J. Manuf. Sci. Technol.* **2020**, *31*, 525–538. [CrossRef]
41. Haghdadi, N.; Laleh, M.; Moyle, M.; Primig, S. Additive Manufacturing of Steels: A Review of Achievements and Challenges. *J. Mater. Sci.* **2021**, *56*, 64–107. [CrossRef]
42. Fedina, T.; Sundqvist, J.; Kaplan, A.F.H. The Use of Non-Spherical Powder Particles in Laser Powder Bed Fusion. *IOP Conf. Ser. Mater. Sci. Eng.* **2021**, *1135*, 012018. [CrossRef]
43. Kruzhanov, V.; Arnhold, V. Energy Consumption in Powder Metallurgical Manufacturing. *Powder Metall.* **2012**, *55*, 14–21. [CrossRef]
44. Martin, J.H.; Barnes, J.E.; Rogers, K.A.; Hundley, J.; LaPlant, D.L.; Ghanbari, S.; Tsai, J.-T.; Bahr, D.F. Additive Manufacturing of a High-Performance Aluminum Alloy from Cold Mechanically Derived Non-Spherical Powder. *Commun. Mater.* **2023**, *4*, 39. [CrossRef]
45. Faludi, J.; Baumers, M.; Maskery, I.; Hague, R. Environmental Impacts of Selective Laser Melting: Do Printer, Powder, Or Power Dominate? *J. Ind. Ecol.* **2017**, *21*, S144–S156. [CrossRef]
46. Tsirlis, M.; Michailidis, N. Optimization of Aluminium Powder Production through a Novel Ultralow Pressure Gas-Atomization Method. *CIRP Ann.* **2022**, *71*, 141–144. [CrossRef]
47. Tsirlis, M.; Michailidis, N. Low-Pressure Gas Atomization of Aluminum through a Venturi Nozzle. *Adv. Powder Technol.* **2020**, *31*, 1720–1727. [CrossRef]
48. Lagutkin, S.; Achelis, L.; Sheikhaliev, S.; Uhlenwinkel, V.; Srivastava, V. Atomization Process for Metal Powder. *Mater. Sci. Eng. A* **2004**, *383*, 1–6. [CrossRef]
49. Neikov, O.D. Atomization and Granulation. In *Handbook of Non-Ferrous Metal Powders*; Elsevier: Amsterdam, The Netherlands, 2019; pp. 125–185.
50. Dunkley, J.J. Advances in Atomisation Techniques for the Formation of Metal Powders. In *Advances in Powder Metallurgy*; Elsevier: Amsterdam, The Netherlands, 2013; pp. 3–18.
51. DirectPowderTM System. Available online: https://www.metalpowderworks.com/technology (accessed on 25 October 2024).
52. Sehhat, M.H.; Chandler, J.; Yates, Z. A Review on ICP Powder Plasma Spheroidization Process Parameters. *Int. J. Refract. Met. Hard Mater.* **2022**, *103*, 105764. [CrossRef]
53. UniMelt Microwave-Based Plasma Technology. Available online: https://www.6kinc.com/6k-inc-unimelt-metal-powders/unimelt-microwave-based-plasma-technology/ (accessed on 30 September 2024).
54. Gao, C.; Wolff, S.; Wang, S. Eco-Friendly Additive Manufacturing of Metals: Energy Efficiency and Life Cycle Analysis. *J. Manuf. Syst.* **2021**, *60*, 459–472. [CrossRef]
55. Sustainability for Advanced Manufacturing. Available online: https://www.continuumpowders.com/sustainability (accessed on 26 September 2024).
56. RePowder-Ultrasonic Powder Atomizer and Alloy Prototyping Platform. Available online: https://www.amazemet.com/repowder/ (accessed on 26 September 2024).
57. Seifeddine, S.; Johansson, S.; Svensson, I.L. The Influence of Cooling Rate and Manganese Content on the β-Al5FeSi Phase Formation and Mechanical Properties of Al–Si-Based Alloys. *Mater. Sci. Eng. A* **2008**, *490*, 385–390. [CrossRef]
58. Petrik, J.; Horvath, M. THE IRON CORRECTORS IN Al-Si ALLOYS. *Ann. Fac. Eng. Hunedoara* **2011**, *9*, 401.
59. Bhatt, B.; Martucci, A.; Virgillito, E.; Gobber, F.; Bondioli, F.; Manfredi, D.; Lombardi, M.; Fino, P. Deciphering Microstructures and Phases of Gas-Atomised Novel Al-Fe-Si-Cr-Ni Alloys. *Metals* **2023**, *14*, 17. [CrossRef]
60. *ASTM F3592-23*; Standard Guide for Additive Manufacturing of Metals-Powder Bed Fusion-Guidelines for Feedstock Re-Use and Sampling Strategies. ASTM International: West Conshohocken, PA, USA, 2023. [CrossRef]
61. Sun, X.; Chen, M.; Liu, T.; Zhang, K.; Wei, H.; Zhu, Z.; Liao, W. Characterization, Preparation, and Reuse of Metallic Powders for Laser Powder Bed Fusion: A Review. *Int. J. Extrem. Manuf.* **2024**, *6*, 012003. [CrossRef]
62. Gasper, A.N.D.; Szost, B.; Wang, X.; Johns, D.; Sharma, S.; Clare, A.T.; Ashcroft, I.A. Spatter and Oxide Formation in Laser Powder Bed Fusion of Inconel 718. *Addit. Manuf.* **2018**, *24*, 446–456. [CrossRef]
63. Cordova, L.; Bor, T.; de Smit, M.; Carmignato, S.; Campos, M.; Tinga, T. Effects of Powder Reuse on the Microstructure and Mechanical Behaviour of Al–Mg–Sc–Zr Alloy Processed by Laser Powder Bed Fusion (LPBF). *Addit. Manuf.* **2020**, *36*, 101625. [CrossRef]
64. *ASTM F3318-18*; Standard for Additive Manufacturing-Finished Part Properties-Specification for AlSi10Mg with Powder Bed Fusion-Laser Beam. ASTM International: West Conshohocken, PA, USA, 2018.
65. Asgari, H.; Baxter, C.; Hosseinkhani, K.; Mohammadi, M. On Microstructure and Mechanical Properties of Additively Manufactured AlSi10Mg_200C Using Recycled Powder. *Mater. Sci. Eng. A* **2017**, *707*, 148–158. [CrossRef]
66. Smolina, I.; Gruber, K.; Pawlak, A.; Ziółkowski, G.; Grochowska, E.; Schob, D.; Kobiela, K.; Roszak, R.; Ziegenhorn, M.; Kurzynowski, T. Influence of the AlSi7Mg0.6 Aluminium Alloy Powder Reuse on the Quality and Mechanical Properties of LPBF Samples. *Materials* **2022**, *15*, 5019. [CrossRef] [PubMed]

67. Reyes Belmonte, M.A.; Copeland, C.D.; Hislop, D.; Hopkins, G.; Schmieder, A.; Bredda, S.; Akehurst, S. Improving Heat Transfer and Reducing Mass in a Gasoline Piston Using Additive Manufacturing. In *SAE Technical Papers*; SAE International: Warrendale, PA, USA, 2015; Volume 2015.
68. Priarone, P.C.; Catalano, A.R.; Settineri, L. Additive Manufacturing for the Automotive Industry: On the Life-Cycle Environmental Implications of Material Substitution and Lightweighting through Re-Design. *Prog. Addit. Manuf.* **2023**, *8*, 1229–1240. [CrossRef]
69. Yap, C.Y.; Chua, C.K.; Dong, Z.L.; Liu, Z.H.; Zhang, D.Q.; Loh, L.E.; Sing, S.L. Review of Selective Laser Melting: Materials and Applications. *Appl. Phys. Rev.* **2015**, *2*, 041101. [CrossRef]
70. Herzog, D.; Seyda, V.; Wycisk, E.; Emmelmann, C. Additive Manufacturing of Metals. *Acta Mater.* **2016**, *117*, 371–392. [CrossRef]
71. Blanco, D.; Rubio, E.M.; Lorente, R.; Sáenz-Nuño, M.A. Lightweight Structural Materials in Open Access: Latest Trends. *Materials* **2021**, *14*, 6577. [CrossRef]
72. Bandivadekar, A.; Bodek, K.; Cheah, L.; Evans, C.; Groode, T.; Heywood, J.; Kasseris, E.; Kromer, M.; Weiss, M. *On the Road in 2035: Reducing Transportation's Petroleum Consumption and GHG Emissions*; Massachusetts Institute of Technology: Cambridge, MA, USA, 2008.
73. Robinson, A.L.; Taub, A.I.; Keoleian, G.A. Fuel Efficiency Drives the Auto Industry to Reduce Vehicle Weight. *MRS Bull.* **2019**, *44*, 920–923. [CrossRef]
74. Zhu, L.; Li, N.; Childs, P.R.N. Light-Weighting in Aerospace Component and System Design. *Propuls. Power Res.* **2018**, *7*, 103–119. [CrossRef]
75. Almussa, N.F.; Almaktoom, A. The Effects of Reducing Aircraft Weight on Profitability and Fuel Consumption. *PalArch's J. Archaeol. Egypt./Egyptol.* **2021**, *18*, 206–214.
76. Marino, M.; Sabatini, R. Advanced Lightweight Aircraft Design Configurations for Green Operations. In Proceedings of the Practical Responses to Climate Change (PRCC), Melbourne, Australia, 25–27 November 2014.
77. Martin, J.H.; Yahata, B.D.; Hundley, J.M.; Mayer, J.A.; Schaedler, T.A.; Pollock, T.M. 3D Printing of High-Strength Aluminium Alloys. *Nature* **2017**, *549*, 365–369. [CrossRef]
78. Mertens, A.; Delahaye, J.; Dedry, O.; Vertruyen, B.; Tchuindjang, J.T.; Habraken, A.M. Microstructure and Properties of SLM AlSi10Mg: Understanding the Influence of the Local Thermal History. *Procedia Manuf.* **2020**, *47*, 1089–1095. [CrossRef]
79. Zhang, X.; Zheng, H.; Yu, W. A Review on Solidification Cracks in High-Strength Aluminum Alloys via Laser Powder Bed Fusion. *Mater. Today Proc.* **2022**, *70*, 465–469. [CrossRef]
80. Hyer, H.; Mehta, A.; Graydon, K.; Kljestan, N.; Knezevic, M.; Weiss, D.; McWilliams, B.; Cho, K.; Sohn, Y. High Strength Aluminum-Cerium Alloy Processed by Laser Powder Bed Fusion. *Addit. Manuf.* **2022**, *52*, 102657. [CrossRef]
81. Aversa, A.; Marchese, G.; Saboori, A.; Bassini, E.; Manfredi, D.; Biamino, S.; Ugues, D.; Fino, P.; Lombardi, M. New Aluminum Alloys Specifically Designed for Laser Powder Bed Fusion: A Review. *Materials* **2019**, *12*, 1007. [CrossRef]
82. Minasyan, T.; Hussainova, I. Laser Powder-Bed Fusion of Ceramic Particulate Reinforced Aluminum Alloys: A Review. *Materials* **2022**, *15*, 2467. [CrossRef] [PubMed]
83. Zhu, Z.; Hu, Z.; Seet, H.L.; Liu, T.; Liao, W.; Ramamurty, U.; Ling Nai, S.M. Recent Progress on the Additive Manufacturing of Aluminum Alloys and Aluminum Matrix Composites: Microstructure, Properties, and Applications. *Int. J. Mach. Tools Manuf.* **2023**, *190*, 104047. [CrossRef]
84. Li, X.; Li, G.; Zhang, M.X.; Zhu, Q. Novel Approach to Additively Manufacture High-Strength Al Alloys by Laser Powder Bed Fusion through Addition of Hybrid Grain Refiners. *Addit. Manuf.* **2021**, *48*, 102400. [CrossRef]
85. The Most Advanced Aluminum Alloy Feedstocks. Available online: https://www.elementum3d.com/aluminum/ (accessed on 23 May 2024).
86. Begoc, S.; Montredon, F.; Pommatau, G.; Leger, G.; Gas, M.; Eyrignoux, S. Additive Manufacturing of Scalmalloy® Satellite Parts. In Proceedings of the 8th European Conference for Aeronautics and Space Sciences (EUCASS 2019), Madrid, Spain, 1–4 July 2019.
87. Zakharov, V.V. Effect of Scandium on the Structure and Properties of Aluminum Alloys. *Met. Sci. Heat. Treat.* **2003**, *45*, 246–253. [CrossRef]
88. Martucci, A.; Aversa, A.; Manfredi, D.; Bondioli, F.; Biamino, S.; Ugues, D.; Lombardi, M.; Fino, P. Low-Power Laser Powder Bed Fusion Processing of Scalmalloy®. *Materials* **2022**, *15*, 3123. [CrossRef]
89. Muhammad, M.; Nezhadfar, P.D.; Thompson, S.; Saharan, A.; Phan, N.; Shamsaei, N. A Comparative Investigation on the Microstructure and Mechanical Properties of Additively Manufactured Aluminum Alloys. *Int. J. Fatigue* **2021**, *146*, 106165. [CrossRef]
90. Ghasri-Khouzani, M.; Karimialavijeh, H.; Pröbstle, M.; Batmaz, R.; Muhammad, W.; Chakraborty, A.; Sabiston, T.D.; Harvey, J.P.; Martin, É. Processability and Characterization of A20X Aluminum Alloy Fabricated by Laser Powder Bed Fusion. *Mater. Today Commun.* **2023**, *35*, 105555. [CrossRef]
91. Aheadd® Aluminium Powders for Additive Manufacturing. Available online: https://www.constellium.com/products/aluminium-powders (accessed on 17 May 2024).

92. Pauzon, C.; Buttard, M.; Després, A.; Chehab, B.; Blandin, J.J.; Martin, G. A Novel Laser Powder Bed Fusion Al-Fe-Zr Alloy for Superior Strength-Conductivity Trade-Off. *Scr. Mater.* **2022**, *219*, 114878. [CrossRef]
93. Pauzon, C.; Buttard, M.; Després, A.; Charlot, F.; Fivel, M.; Chehab, B.; Blandin, J.J.; Martin, G. Direct Ageing of LPBF Al-1Fe-1Zr for High Conductivity and Mechanical Performance. *Acta Mater.* **2023**, *258*, 119199. [CrossRef]
94. Gong, J.; Wei, K.; Liu, M.; Song, W.; Li, X.; Zeng, X. Microstructure and Mechanical Properties of AlSi10Mg Alloy Built by Laser Powder Bed Fusion/Direct Energy Deposition Hybrid Laser Additive Manufacturing. *Addit. Manuf.* **2022**, *59*, 103160. [CrossRef]
95. Bassoli, E.; Tognoli, E.; Defanti, S. High-Temperature Tensile Behavior of AlSi7Mg Parts Built by LPBF under High-Productivity Conditions. *Prog. Addit. Manuf.* **2024**, *9*, 2413–2426. [CrossRef]
96. Kimura, M.; Hirayama, A.; Yoshioka, J.; Maekawa, H.; Kusaka, M.; Kaizu, K.; Takahashi, T. Mechanical Properties of AlSi12 Alloy Manufactured by Laser Powder Bed Fusion Technique. *J. Fail. Anal. Prev.* **2020**, *20*, 1884–1895. [CrossRef]
97. Uddin, S.Z.; Murr, L.E.; Terrazas, C.A.; Morton, P.; Roberson, D.A.; Wicker, R.B. Processing and Characterization of Crack-Free Aluminum 6061 Using High-Temperature Heating in Laser Powder Bed Fusion Additive Manufacturing. *Addit. Manuf.* **2018**, *22*, 405–415. [CrossRef]
98. Chen, Y.; Xiao, C.; Zhu, S.; Li, Z.; Yang, W.; Zhao, F.; Yu, S.; Shi, Y. Microstructure Characterization and Mechanical Properties of Crack-Free Al-Cu-Mg-Y Alloy Fabricated by Laser Powder Bed Fusion. *Addit. Manuf.* **2022**, *58*, 103006. [CrossRef]
99. Montero Sistiaga, M.L.; Mertens, R.; Vrancken, B.; Wang, X.; Van Hooreweder, B.; Kruth, J.P.; Van Humbeeck, J. Changing the Alloy Composition of Al7075 for Better Processability by Selective Laser Melting. *J. Mater. Process Technol.* **2016**, *238*, 437–445. [CrossRef]
100. High-Performance Aluminium for Additive Manufacturing. Available online: https://www.fehrmann-materials.com/en/metal-powder (accessed on 1 September 2024).
101. Sun, Z.; Wang, H.; Tian, X.; He, B. Developing a Novel Lightweight Al–Mg–Li Alloy for Laser Powder Bed Fusion Additive Manufacturing: Parameter Optimization, Microstructure Evolution, and Mechanical Performance. *Mater. Sci. Eng. A* **2023**, *872*, 144992. [CrossRef]
102. Zhou, L.; Pan, H.; Hyer, H.; Park, S.; Bai, Y.; McWilliams, B.; Cho, K.; Sohn, Y. Microstructure and Tensile Property of a Novel AlZnMgScZr Alloy Additively Manufactured by Gas Atomization and Laser Powder Bed Fusion. *Scr. Mater.* **2019**, *158*, 24–28. [CrossRef]
103. Trujillo-Tadeo, J.J.; Arruebarrena, G.; Dorantes-Rosales, H.J.; Bilbao, Y.; Vicario, I.; Guraya, T.; Hurtado, I. Design and Characterization of a Novel Lightweight Multicomponent Alloy Al58Zn28Mg6Si8. *J. Mater. Res. Technol.* **2023**, *27*, 3751–3760. [CrossRef]
104. Chang, K.-C.; Zhao, J.-R.; Hung, F.-Y. Microstructure, Mechanical Properties, and Fatigue Fracture Characteristics of High-Fracture-Resistance Selective Laser Melting Al-Ni-Cu Alloys. *Metals* **2021**, *11*, 87. [CrossRef]
105. Lučić, M.; Lukić, J.; Grujić, I. Statistical Analysis of Trends in Battery Electric Vehicles: Special Reference to Vehicle Weight Reduction, Electric Motor, Battery, and Interior Space Dimensions. *Arch. Automot. Eng.—Arch. Motoryz.* **2024**, *104*, 63–96. [CrossRef]
106. Sigmund, O.; Maute, K. Topology Optimization Approaches. *Struct. Multidiscip. Optim.* **2013**, *48*, 1031–1055. [CrossRef]
107. Suzuki, K.; Kikuchi, N. A Homogenization Method for Shape and Topology Optimization. *Comput. Methods Appl. Mech. Eng.* **1991**, *93*, 291–318. [CrossRef]
108. Bendsøe, M.P.; Kikuchi, N. Generating optimal topologies in structural design using a homogenization method. *Comput. Methods Appl. Mech. Eng.* **1988**, *71*, 197–224. [CrossRef]
109. Bendsøe, M.P. Optimal Shape Design as a Material Distribution Problem. *Struct. Optim.* **1989**, *1*, 193–202. [CrossRef]
110. Tajima, M.; Yamada, T. Topology Optimization with Geometric Constraints for Additive Manufacturing Based on Coupled Fictitious Physical Model. *Comput. Methods Appl. Mech. Eng.* **2023**, *417*, 116415. [CrossRef]
111. Ahmad, A.; Bici, M.; Campana, F. Guidelines for Topology Optimization as Concept Design Tool and Their Application for the Mechanical Design of the Inner Frame to Support an Ancient Bronze Statue. *Appl. Sci.* **2021**, *11*, 7834. [CrossRef]
112. Larsson, R. Methodology for Topology and Shape Optimization: Application to a Rear Lower Control Arm. Master's Thesis, Chalmers University of Technology, Gothenburg, Sweden, 2016.
113. Van De Ven, E.A. Topology Optimization for Additive Manufacturing: A Front Propagation-Based Approach. Ph.D. Thesis, Delft University of Technology, Delft, The Netherlands, 2021.
114. Karimzadeh, R.; Hamedi, M. An Intelligent Algorithm for Topology Optimization in Additive Manufacturing. *Int. J. Adv. Manuf. Technol.* **2022**, *119*, 991–1001. [CrossRef]
115. Zhu, J.; Zhou, H.; Wang, C.; Zhou, L.; Yuan, S.; Zhang, W. A Review of Topology Optimization for Additive Manufacturing: Status and Challenges. *Chin. J. Aeronaut.* **2021**, *34*, 91–110. [CrossRef]
116. Mansor, W.; Muhamad, W.; Reshid, M.; Wahid, K.; Nur, M.; Saniman, F.; Muhamad, W.M.W.; Wahid, K.A.A.; Reshid, M.N. Mass Reduction of a Jet Engine Bracket Using Topology Optimisation for Additive Manufacturing Application. *Int. J. Adv. Sci. Technol.* **2020**, *29*, 4438–4444.

117. Berrocal, L.; Fernández, R.; González, S.; Periñán, A.; Tudela, S.; Vilanova, J.; Rubio, L.; Martín Márquez, J.M.; Guerrero, J.; Lasagni, F. Topology Optimization and Additive Manufacturing for Aerospace Components. *Prog. Addit. Manuf.* **2019**, *4*, 83–95. [CrossRef]
118. Tyflopoulos, E.; Lien, M.; Steinert, M. Optimization of Brake Calipers Using Topology Optimization for Additive Manufacturing. *Appl. Sci.* **2021**, *11*, 1437. [CrossRef]
119. Mantovani, S.; Barbieri, S.G.; Giacopini, M.; Croce, A.; Sola, A.; Bassoli, E. Synergy between Topology Optimization and Additive Manufacturing in the Automotive Field. *Proc. Inst. Mech. Eng. B J. Eng. Manuf.* **2021**, *235*, 555–567. [CrossRef]
120. Kim, G.-W.; Park, Y.-I.; Park, K. Topology Optimization and Additive Manufacturing of Automotive Component by Coupling Kinetic And Structural Analyses. *Int. J. Automot. Technol.* **2020**, *21*, 1455–1463. [CrossRef]
121. Journey of the Light Rider. Available online: https://www.apworks.de/blog-lightrider (accessed on 2 May 2024).
122. Antenna Bracket for RUAG's Sentinel Satellite. Available online: https://uk.eos.info/en-gb/innovations/all-3d-printing-applications/aerospace/aerospace-case-studies/ruag-aerospace-3d-printed-satellite-components (accessed on 4 May 2024).
123. Victoria Burt 3D-Printed Satellite Component Presents a Lesson in Rethinking Design. Available online: https://altairengineering.it/c2r/ws2016/3d-printed-satellite-component-presents-lesson-rethinking-design (accessed on 4 May 2024).
124. Barthelat, F. Architectured Materials in Engineering and Biology: Fabrication, Structure, Mechanics and Performance. *Int. Mater. Rev.* **2015**, *60*, 413–430. [CrossRef]
125. Babaee, S.; Shim, J.; Weaver, J.C.; Chen, E.R.; Patel, N.; Bertoldi, K. 3D Soft Metamaterials with Negative Poisson's Ratio. *Adv. Mater.* **2013**, *25*, 5044–5049. [CrossRef]
126. Chen, D.; Zheng, X. Multi-Material Additive Manufacturing of Metamaterials with Giant, Tailorable Negative Poisson's Ratios. *Sci. Rep.* **2018**, *8*, 9139. [CrossRef] [PubMed]
127. Mahmoud, D.; Tandel, S.R.S.; Yakout, M.; Elbestawi, M.; Mattiello, F.; Paradiso, S.; Ching, C.; Zaher, M.; Abdelnabi, M. Enhancement of Heat Exchanger Performance Using Additive Manufacturing of Gyroid Lattice Structures. *Int. J. Adv. Manuf. Technol.* **2023**, *126*, 4021–4036. [CrossRef]
128. Kladovasilakis, N.; Tsongas, K.; Tzetzis, D. Finite Element Analysis of Orthopedic Hip Implant with Functionally Graded Bioinspired Lattice Structures. *Biomimetics* **2020**, *5*, 44. [CrossRef]
129. Jafarabadi, A.; Ferretto, I.; Mohri, M.; Leinenbach, C.; Ghafoori, E. 4D Printing of Recoverable Buckling-Induced Architected Iron-Based Shape Memory Alloys. *Mater. Des.* **2023**, *233*, 112216. [CrossRef]
130. Nandhakumar, R.; Venkatesan, K. A Process Parameters Review on Selective Laser Melting-Based Additive Manufacturing of Single and Multi-Material: Microstructure, Physical Properties, Tribological, and Surface Roughness. *Mater. Today Commun.* **2023**, *35*, 105538. [CrossRef]
131. Martucci, A.; Aversa, A.; Lombardi, M. Ongoing Challenges of Laser-Based Powder Bed Fusion Processing of Al Alloys and Potential Solutions from the Literature—A Review. *Materials* **2023**, *16*, 1084. [CrossRef]
132. Benedetti, B.; Caponigro, V.; Ardini, F. Experimental Design Step by Step: A Practical Guide for Beginners. *Crit. Rev. Anal. Chem.* **2022**, *52*, 1015–1028. [CrossRef]
133. Rao, R.V. *Advanced Modeling and Optimization of Manufacturing Processes*; Springer Series in Advanced Manufacturing; Springer: London, UK, 2011; ISBN 978-0-85729-014-4.
134. Montgomery, D.C. *Design and Analysis of Experiments*; John Wiley & Sons: Hoboken, NJ, USA, 2010; ISBN 9781119113478.
135. Leardi, R. Experimental Design. In *Data Handling in Science and Technology*; Elsevier Ltd.: Amsterdam, The Netherlands, 2013; Volume 28, pp. 9–53.
136. Tanco, M.; Viles, E.; Pozueta, L. *Comparing Different Approaches for Design of Experiments (DoE)*; Lecture Notes in Electrical Engineering; Springer: Dordrecht, The Netherlands, 2009; Volume 39, pp. 611–621.
137. Jankovic, A.; Chaudhary, G.; Goia, F. Designing the Design of Experiments (DOE)—An Investigation on the Influence of Different Factorial Designs on the Characterization of Complex Systems. *Energy Build.* **2021**, *250*, 111298. [CrossRef]
138. Majeed, A.; Lv, J.; Majeed, A.; Zhang, Y.F.; Lv, J.X.; Peng, T.; Waqar, S.; Atta, Z. Study the Effect of Heat Treatment on the Relative Density of SLM Built Parts of AlSi10Mg Alloy. In Proceedings of the 48th international conference on computers and industrial engineering (CIE 2018), Auckland, New Zealand, 2–5 December 2018.
139. Majeed, A.; Lv, J.; Zhang, Y.; Muzamil, M.; Waqas, A.; Shamim, K.; Qureshi, M.E.; Zafar, F. An Investigation into the Influence of Processing Parameters on the Surface Quality of AlSi10Mg Parts by SLM Process. In Proceedings of the 2019 16th International Bhurban Conference on Applied Sciences and Technology (IBCAST), Islamabad, Pakistan, 8–12 January 2019; IEEE: Piscataway, NJ, USA, 2019; pp. 143–147.
140. Leal, M.L.B.; Bermudez-Reyes, B.; Del Carmen Zambrano Robledo, P.; Lopez-Botello, O. Parameter Optimization of Aluminum Alloy Thin Structures Obtained by Selective Laser Melting. *MRS Adv.* **2019**, *4*, 2997–3005. [CrossRef]
141. Maamoun, A.H.; Xue, Y.F.; Elbestawi, M.A.; Veldhuis, S.C. Effect of Selective Laser Melting Process Parameters on the Quality of al Alloy Parts: Powder Characterization, Density, Surface Roughness, and Dimensional Accuracy. *Materials* **2018**, *11*, 2343. [CrossRef]

142. Aversa, A.; Moshiri, M.; Librera, E.; Hadi, M.; Marchese, G.; Manfredi, D.; Lorusso, M.; Calignano, F.; Biamino, S.; Lombardi, M.; et al. Single Scan Track Analyses on Aluminium Based Powders. *J. Mater. Process Technol.* **2018**, *255*, 17–25. [CrossRef]
143. Martucci, A.; Marinucci, F.; Sivo, A.; Aversa, A.; Manfredi, D.; Bondioli, F.; Fino, P.; Lombardi, M. An Automatic on Top Analysis of Single Scan Tracks to Evaluate the Laser Powder Bed Fusion Building Parameters. *Materials* **2021**, *14*, 5171. [CrossRef]
144. Marola, S.; Gianoglio, D.; Bosio, F.; Aversa, A.; Lorusso, M.; Manfredi, D.; Lombardi, M.; Battezzati, L. Alloying AlSi10Mg and Cu Powders in Laser Single Scan Tracks, Melt Spinning, and Laser Powder Bed Fusion. *J. Alloys Compd.* **2020**, *821*, 153538. [CrossRef]
145. Bosio, F.; Aversa, A.; Lorusso, M.; Marola, S.; Gianoglio, D.; Battezzati, L.; Fino, P.; Manfredi, D.; Lombardi, M. A Time-Saving and Cost-Effective Method to Process Alloys by Laser Powder Bed Fusion. *Mater. Des.* **2019**, *181*, 107949. [CrossRef]
146. Gheysen, J.; Marteleur, M.; van der Rest, C.; Simar, A. Efficient Optimization Methodology for Laser Powder Bed Fusion Parameters to Manufacture Dense and Mechanically Sound Parts Validated on AlSi12 Alloy. *Mater. Des.* **2021**, *199*, 109433. [CrossRef]
147. Wang, P.; Robertson, G.; Gibson, B.T.; Fancher, C.M.; Reynolds, J.; Borish, M.; Cruz, J.R.; Chesser, P.; Stump, B.; Jackson, A.; et al. Improved Productivity with Multilaser Rotary Powder Bed Fusion Additive Manufacturing. *3D Print. Addit. Manuf.* **2024**, *11*, 231–241. [CrossRef]
148. Gutowski, T.; Jiang, S.; Cooper, D.; Corman, G.; Hausmann, M.; Manson, J.; Schudeleit, T.; Wegener, K.; Sabelle, M.; Ramos-Grez, J.; et al. Note on the Rate and Energy Efficiency Limits for Additive Manufacturing. *J. Ind. Ecol.* **2017**, *21*, S69–S79. [CrossRef]
149. Kasprowicz, M.; Pawlak, A.; Jurkowski, P.; Kurzynowski, T. Ways to Increase the Productivity of L-PBF Processes. *Arch. Civ. Mech. Eng.* **2023**, *23*, 211. [CrossRef]
150. Tang, M.; Pistorius, P.C.; Montgomery, C.; Beuth, J. Build Rate Optimization for Powder Bed Fusion. *J. Mater. Eng. Perform.* **2019**, *28*, 641–647. [CrossRef]
151. King, W.E.; Barth, H.D.; Castillo, V.M.; Gallegos, G.F.; Gibbs, J.W.; Hahn, D.E.; Kamath, C.; Rubenchik, A.M. Observation of Keyhole-Mode Laser Melting in Laser Powder-Bed Fusion Additive Manufacturing. *J. Mater. Process Technol.* **2014**, *214*, 2915–2925. [CrossRef]
152. Taghian, M.; Mosallanejad, M.H.; Lannunziata, E.; Del Greco, G.; Iuliano, L.; Saboori, A. Laser Powder Bed Fusion of Metallic Components: Latest Progress in Productivity, Quality, and Cost Perspectives. *J. Mater. Res. Technol.* **2023**, *27*, 6484–6500. [CrossRef]
153. Defanti, S.; Cappelletti, C.; Gatto, A.; Tognoli, E.; Fabbri, F. Boosting Productivity of Laser Powder Bed Fusion for AlSi10Mg. *J. Manuf. Mater. Process.* **2022**, *6*, 112. [CrossRef]
154. Vaudreuil, S.; Bencaid, S.E.; Vanaei, H.R.; El Magri, A. Effects of Power and Laser Speed on the Mechanical Properties of AlSi7Mg0.6 Manufactured by Laser Powder Bed Fusion. *Materials* **2022**, *15*, 8640. [CrossRef] [PubMed]
155. Mercurio, V.; Calignano, F.; Viccica, M.; Iuliano, L. Increasing of Production Rate of Laser Powder Bed Fusion Systems. *Procedia CIRP* **2023**, *118*, 699–704. [CrossRef]
156. EOS M 400—3D Printing for Industrial Production | EOS GmbH. Available online: https://www.eos.info/en-us/metal-solutions/metal-printers/eos-m-400 (accessed on 28 August 2024).
157. Carter, W.T.; Graham, M.E.; Hayden, C.J.; Jeong, Y.; Mamrak, J.; McCarthy, B.S.; Monaghan, W.F.; Nieters, E.J.; Ostroverkhov, V.; Roychowdhury, S.; et al. A Large Format DMLM System Using a Continuously Rotating Powder Bed. *Addit. Manuf.* **2020**, *31*, 100983. [CrossRef]
158. Hauser, C.; Sutcliffe, C.; Egan, M.; Fox MSERC, P. Spiral Growth Manufacturing (SGM)—A Continuous Additive Manufacturing Technology for Processing Metal Powder by Selective Laser Melting. In Proceedings of the 2005 International Solid Freeform Fabrication Symposium, Austin, TX, USA, 1–3 August 2005.
159. Stump, B.C.; Gibson, B.T.; Reynolds, J.T.; Wade, C.C.; Borish, M.C.; Wang, P.L. Load Balancing for Multi-Beam Additive Manufacturing Systems. *Addit. Manuf.* **2023**, *74*, 103708. [CrossRef]
160. Ramos-Grez, J.A.; Norambuena, M.L.; Pérez, I.J.; Saavedra, D.G.; Aguilera, M.G. Development of Powder Bed Laser 3D Printing in Polar Coordinates and Its Comparison with Conventional Cartesian Laser 3D Printing. In *XV Ibero-American Congress of Mechanical Engineering*; Springer International Publishing: Cham, Switzerland, 2023; pp. 362–368.
161. Du Plessis, A.; Yelamanchi, B.; Fischer, C.; Miller, J.; Beamer, C.; Rogers, K.; Cortes, P.; Els, J.; MacDonald, E. Productivity Enhancement of Laser Powder Bed Fusion Using Compensated Shelled Geometries and Hot Isostatic Pressing. *Adv. Ind. Manuf. Eng.* **2021**, *2*, 100031. [CrossRef]
162. Yim, S.; Bian, H.; Aoyagi, K.; Yamanaka, K.; Chiba, A. Effect of Powder Morphology on Flowability and Spreading Behavior in Powder Bed Fusion Additive Manufacturing Process: A Particle-Scale Modeling Study. *Addit. Manuf.* **2023**, *72*, 103612. [CrossRef]
163. Cacace, S.; Semeraro, Q. Fast Optimisation Procedure for the Selection of L-PBF Parameters Based on Utility Function. *Virtual Phys. Prototyp.* **2022**, *17*, 125–137. [CrossRef]
164. Toyserkani, E.; Sarker, D.; Ibhadode, O.O.; Liravi, F.; Russo, P.; Taherkhani, K. Monitoring and Quality Assurance for Metal Additive Manufacturing. In *Metal Additive Manufacturing*; Wiley: Hoboken, NJ, USA, 2021; pp. 507–575.

165. DebRoy, T.; Wei, H.L.; Zuback, J.S.; Mukherjee, T.; Elmer, J.W.; Milewski, J.O.; Beese, A.M.; Wilson-Heid, A.; De, A.; Zhang, W. Additive Manufacturing of Metallic Components—Process, Structure and Properties. *Prog. Mater. Sci.* **2018**, *92*, 112–224. [CrossRef]
166. Leirmo, J.L.; Baturynska, I. Challenges and Proposed Solutions for Aluminium in Laser Powder Bed Fusion. *Procedia CIRP* **2020**, *93*, 114–119. [CrossRef]
167. Zhang, J.; Song, B.; Wei, Q.; Bourell, D.; Shi, Y. A Review of Selective Laser Melting of Aluminum Alloys: Processing, Microstructure, Property and Developing Trends. *J. Mater. Sci. Technol.* **2019**, *35*, 270–284. [CrossRef]
168. Zhang, H.; Vallabh, C.K.P.; Zhao, X. Registration and Fusion of Large-Scale Melt Pool Temperature and Morphology Monitoring Data Demonstrated for Surface Topography Prediction in LPBF. *Addit. Manuf.* **2022**, *58*, 103075. [CrossRef]
169. Rees, D.T.; Leung, C.L.A.; Elambasseril, J.; Marussi, S.; Shah, S.; Marathe, S.; Brandt, M.; Easton, M.; Lee, P.D. In Situ X-Ray Imaging of Hot Cracking and Porosity during LPBF of Al-2139 with TiB2 Additions and Varied Process Parameters. *Mater. Des.* **2023**, *231*, 112031. [CrossRef]
170. Pagani, L.; Grasso, M.; Scott, P.J.; Colosimo, B.M. Automated Layerwise Detection of Geometrical Distortions in Laser Powder Bed Fusion. *Addit. Manuf.* **2020**, *36*, 101435. [CrossRef]
171. Liu, D.; Li, X.; Su, Y.; Guo, J.; Luo, L.; Fu, H. Influence of Initial Solid–Liquid Interface Morphology on Further Microstructure Evolution during Directional Solidification. *Appl. Phys. A* **2013**, *110*, 443–451. [CrossRef]
172. Tang, Y.; Xiao, D.; Huang, L.; You, R.; Zhao, X.; Lin, N.; Ma, Y.; Liu, W. Effect of Minor Sc Addition on the Microstructure Evolution of Al–Cu–Li–Mg Alloy During Homogenization with Different Cooling Modes. *Met. Mater. Int.* **2022**, *28*, 2422–2433. [CrossRef]
173. Schmeiser, F.; Krohmer, E.; Wagner, C.; Schell, N.; Uhlmann, E.; Reimers, W. In Situ Microstructure Analysis of Inconel 625 during Laser Powder Bed Fusion. *J. Mater. Sci.* **2022**, *57*, 9663–9677. [CrossRef]
174. Craeghs, T.; Bechmann, F.; Berumen, S.; Kruth, J.-P. Feedback Control of Layerwise Laser Melting Using Optical Sensors. *Phys. Procedia* **2010**, *5*, 505–514. [CrossRef]
175. Grasso, M.; Colosimo, B.M. Process Defects and in Situ Monitoring Methods in Metal Powder Bed Fusion: A Review. *Meas. Sci. Technol.* **2017**, *28*, 044005. [CrossRef]
176. Fiocchi, J.; Tuissi, A.; Biffi, C.A. Heat Treatment of Aluminium Alloys Produced by Laser Powder Bed Fusion: A Review. *Mater. Des.* **2021**, *204*, 109651. [CrossRef]
177. Qin, H.; Dong, Q.; Fallah, V.; Daymond, M.R. Rapid Solidification and Non-Equilibrium Phase Constitution in Laser Powder Bed Fusion (LPBF) of AlSi10Mg Alloy: Analysis of Nano-Precipitates, Eutectic Phases, and Hardness Evolution. *Metall. Mater. Trans. A* **2020**, *51*, 448–466. [CrossRef]
178. Babu, A.P.; Huang, A.; Birbilis, N. On the Heat Treatment and Mechanical Properties of a High Solute Al–Zn–Mg Alloy Processed through Laser Powder Bed Fusion Process. *Mater. Sci. Eng. A* **2021**, *807*, 140857. [CrossRef]
179. Jia, Q.; Rometsch, P.; Kürnsteiner, P.; Chao, Q.; Huang, A.; Weyland, M.; Bourgeois, L.; Wu, X. Selective Laser Melting of a High Strength Al Mn Sc Alloy: Alloy Design and Strengthening Mechanisms. *Acta Mater.* **2019**, *171*, 108–118. [CrossRef]
180. Martucci, A.; Mehta, B.; Lombardi, M.; Nyborg, L. The Influence of Processing Parameters on the Al-Mn Enriched Nano-Precipitates Formation in a Novel Al-Mn-Cr-Zr Alloy Tailored for Power Bed Fusion-Laser Beam Process. *Metals* **2022**, *12*, 1387. [CrossRef]
181. Aversa, A.; Lorusso, M.; Trevisan, F.; Ambrosio, E.P.; Calignano, F.; Manfredi, D.; Biamino, S.; Fino, P.; Lombardi, M.; Pavese, M. Effect of Process and Post-Process Conditions on the Mechanical Properties of an A357 Alloy Produced via Laser Powder Bed Fusion. *Metals* **2017**, *7*, 68. [CrossRef]
182. Yang, K.V.; Rometsch, P.; Davies, C.H.J.; Huang, A.; Wu, X. Effect of Heat Treatment on the Microstructure and Anisotropy in Mechanical Properties of A357 Alloy Produced by Selective Laser Melting. *Mater. Des.* **2018**, *154*, 275–290. [CrossRef]
183. Schmidtke, K.; Palm, F.; Hawkins, A.; Emmelmann, C. Process and Mechanical Properties: Applicability of a Scandium Modified Al-Alloy for Laser Additive Manufacturing. *Phys. Procedia* **2011**, *12*, 369–374. [CrossRef]
184. Ma, R.; Peng, C.; Cai, Z.; Wang, R.; Zhou, Z.; Li, X.; Cao, X. Manipulating the Microstructure and Tensile Properties of Selective Laser Melted Al–Mg-Sc-Zr Alloy through Heat Treatment. *J. Alloys Compd.* **2020**, *831*, 154773. [CrossRef]
185. Fousová, M.; Dvorský, D.; Michalcová, A.; Vojtěch, D. Changes in the Microstructure and Mechanical Properties of Additively Manufactured AlSi10Mg Alloy after Exposure to Elevated Temperatures. *Mater. Charact.* **2018**, *137*, 119–126. [CrossRef]
186. Oliveira de Menezes, J.T.; Castrodeza, E.M.; Casati, R. Effect of Build Orientation on Fracture and Tensile Behavior of A357 Al Alloy Processed by Selective Laser Melting. *Mater. Sci. Eng. A* **2019**, *766*, 138392. [CrossRef]
187. Raffeis, I.; Adjei-Kyeremeh, F.; Vroomen, U.; Richter, S.; Bührig-Polaczek, A. Characterising the Microstructure of an Additively Built Al-Cu-Li Alloy. *Materials* **2020**, *13*, 5188. [CrossRef] [PubMed]
188. Bosio, F.; Phutela, C.; Ghisi, N.; Alhammadi, A.; Aboulkhair, N.T. Tuning the Microstructure and Mechanical Properties of AlSi10Mg Alloy via In-Situ Heat-Treatments in Laser Powder Bed Fusion. *Mater. Sci. Eng. A* **2023**, *879*, 145268. [CrossRef]

189. Schimbäck, D.; Kaserer, L.; Mair, P.; Mohebbi, M.S.; Staron, P.; Maier-Kiener, V.; Letofsky-Papst, I.; Kremmer, T.; Palm, F.; Montes, I.; et al. Advancements in Metal Additive Manufacturing: In-Situ Heat Treatment of Aluminium Alloys during the Laser Powder Bed Fusion Process. *Mater. Sci. Eng. A* **2024**, *905*, 146102. [CrossRef]
190. Rometsch, P.A.; Zhu, Y.; Wu, X.; Huang, A. Review of High-Strength Aluminium Alloys for Additive Manufacturing by Laser Powder Bed Fusion. *Mater. Des.* **2022**, *219*, 110779. [CrossRef]
191. Vanzetti, M.; Virgillito, E.; Aversa, A.; Manfredi, D.; Bondioli, F.; Lombardi, M.; Fino, P. Short Heat Treatments for the F357 Aluminum Alloy Processed by Laser Powder Bed Fusion. *Materials* **2021**, *14*, 6157. [CrossRef] [PubMed]
192. Di Egidio, G.; Ceschini, L.; Morri, A.; Martini, C.; Merlin, M. A Novel T6 Rapid Heat Treatment for AlSi10Mg Alloy Produced by Laser-Based Powder Bed Fusion: Comparison with T5 and Conventional T6 Heat Treatments. *Metall. Mater. Trans. B Process Metall. Mater. Process. Sci.* **2022**, *53*, 284–303. [CrossRef]
193. Laleh, M.; Sadeghi, E.; Revilla, R.I.; Chao, Q.; Haghdadi, N.; Hughes, A.E.; Xu, W.; De Graeve, I.; Qian, M.; Gibson, I.; et al. Heat Treatment for Metal Additive Manufacturing. *Prog. Mater. Sci.* **2023**, *133*, 371–392. [CrossRef]
194. Elementum 3D Launches New High-Strength Aluminum Alloy That Eliminates the Need for Heat Treatment. Available online: https://www.elementum3d.com/elementum-3d-launches-new-high-strength-aluminum-alloy-that-eliminates-the-need-for-heat-treatment/ (accessed on 14 September 2024).
195. Obilanade, D.; Dordlofva, C.; Törlind, P. Surface Roughness Considerations in Design for Additive Manufacturing—A Literature Review. *Proc. Des. Soc.* **2021**, *1*, 2841–2850. [CrossRef]
196. Calignano, F.; Manfredi, D.; Ambrosio, E.P.; Iuliano, L.; Fino, P. Influence of Process Parameters on Surface Roughness of Aluminum Parts Produced by DMLS. *Int. J. Adv. Manuf. Technol.* **2013**, *67*, 2743–2751. [CrossRef]
197. Rao, J.H.; Zhang, K.; Rometsch, P.; Huang, A.; Wu, X. The Influence of Surface Roughness on the Fatigue Performance of Selective Laser Melted Aluminium Alloy A357. In Proceedings of the 16th International Aluminum Alloys Conference, Montreal, QC, Canada, 17–21 June 2018.
198. Ye, C.; Zhang, C.; Zhao, J.; Dong, Y. Effects of Post-Processing on the Surface Finish, Porosity, Residual Stresses, and Fatigue Performance of Additive Manufactured Metals: A Review. *J. Mater. Eng. Perform.* **2021**, *30*, 6407–6425. [CrossRef] [PubMed]
199. Reiber, T.; Rüdesheim, J.; Weigold, M.; Abele, E.; Musekamp, J.; Oechsner, M. Influence of Contour Scans on Surface Roughness and Pore Formation Using Scalmalloy® Manufactured by Laser Powder Bed Fusion (PBF-LB). *Materwiss Werksttech* **2021**, *52*, 468–481. [CrossRef]
200. Strano, G.; Hao, L.; Everson, R.M.; Evans, K.E. Surface Roughness Analysis, Modelling and Prediction in Selective Laser Melting. *J. Mater. Process Technol.* **2013**, *213*, 589–597. [CrossRef]
201. Gadelmawla, E.S.; Koura, M.M.; Maksoud, T.M.A.; Elewa, I.M.; Soliman, H.H. Roughness Parameters. *J. Mater. Process. Technol.* **2002**, *123*, 133–145. [CrossRef]
202. Li, G.; Li, X.; Guo, C.; Zhou, Y.; Tan, Q.; Qu, W.; Li, X.; Hu, X.; Zhang, M.X.; Zhu, Q. Investigation into the Effect of Energy Density on Densification, Surface Roughness and Loss of Alloying Elements of 7075 Aluminium Alloy Processed by Laser Powder Bed Fusion. *Opt. Laser Technol.* **2022**, *147*, 107621. [CrossRef]
203. Li, B.Q.; Li, Z.; Bai, P.; Liu, B.; Kuai, Z. Research on Surface Roughness of AlSi10Mg Parts Fabricated by Laser Powder Bed Fusion. *Metals* **2018**, *8*, 524. [CrossRef]
204. Dhillon, J.S.; Su, S.; Sanchez Mata, O.; Ramakrishnan, T.; Brochu, M. Surface Roughness Studies on F357 Aluminum Alloy Fabricated Using Laser Powder Bed Fusion Process. *Eng. Proc.* **2023**, *43*, 8. [CrossRef]
205. Musekamp, J.; Reiber, T.; Hoche, H.C.; Oechsner, M.; Weigold, M.; Abele, E. Influence of LPBF-surface Characteristics on Fatigue Properties of Scalmalloy®. *Metals* **2021**, *11*, 1961. [CrossRef]
206. Yang, T.; Liu, T.; Liao, W.; Wei, H.; Zhang, C.; Chen, X.; Zhang, K. Effect of Processing Parameters on Overhanging Surface Roughness during Laser Powder Bed Fusion of AlSi10Mg. *J. Manuf. Process* **2021**, *61*, 440–453. [CrossRef]
207. Cao, L.; Li, J.; Hu, J.; Liu, H.; Wu, Y.; Zhou, Q. Optimization of Surface Roughness and Dimensional Accuracy in LPBF Additive Manufacturing. *Opt. Laser Technol.* **2021**, *142*, 107246. [CrossRef]
208. Wang, D.; Liu, Y.; Yang, Y.; Xiao, D. Theoretical and Experimental Study on Surface Roughness of 316L Stainless Steel Metal Parts Obtained through Selective Laser Melting. *Rapid Prototyp. J.* **2016**, *22*, 706–716. [CrossRef]
209. Liu, C.; Yan, D.; Tan, J.; Mai, Z.; Cai, Z.; Dai, Y.; Jiang, M.; Wang, P.; Liu, Z.; Li, C.C.; et al. Development and Experimental Validation of a Hybrid Selective Laser Melting and CNC Milling System. *Addit. Manuf.* **2020**, *36*, 101550. [CrossRef]
210. Zeng, H.; Liu, F.C.; Zhu, S.Z.; Wang, Q.Z.; Wang, Y.D.; Xue, P.; Wu, L.H.; Zhang, H.; Ni, D.R.; Xiao, B.L.; et al. Hybrid Additive Manufacturing of Aluminum Matrix Composites with Improved Mechanical Properties Compared to Extruded Counterparts. *Compos. B Eng.* **2024**, *280*, 111497. [CrossRef]
211. Chu, W.S.; Kim, C.S.; Lee, H.T.; Choi, J.O.; Park, J.I.; Song, J.H.; Jang, K.H.; Ahn, S.H. Hybrid Manufacturing in Micro/Nano Scale: A Review. *Int. J. Precis. Eng. Manuf.—Green. Technol.* **2014**, *1*, 75–92. [CrossRef]
212. Altıparmak, S.C.; Yardley, V.A.; Shi, Z.; Lin, J. Challenges in Additive Manufacturing of High-Strength Aluminium Alloys and Current Developments in Hybrid Additive Manufacturing. *Int. J. Lightweight Mater. Manuf.* **2021**, *4*, 246–261. [CrossRef]

213. Sebbe, N.P.V.; Fernandes, F.; Sousa, V.F.C.; Silva, F.J.G. Hybrid Manufacturing Processes Used in the Production of Complex Parts: A Comprehensive Review. *Metals* **2022**, *12*, 1874. [CrossRef]
214. Matsuura Machinery Corporation. (n.d.). Hybrid Metal 3D Printer LUMEX Series. 17 February 2025. Available online: https://www.lumex-matsuura.com/ (accessed on 18 September 2024).
215. OPM Series. Available online: https://sodick.com/machines/metal-3d-printing/ (accessed on 18 September 2024).
216. Krimpenis, A.A.; Noeas, G.D. Application of Hybrid Manufacturing Processes in Microfabrication. *J. Manuf. Process.* **2022**, *80*, 328–346. [CrossRef]